Published as: Carroll, M.L., B. Johnson, G.A. Henkes, K.W. McMahon, A. Voronkov, W.G. Ambrose Jr., S.G. Denisenko. 2009. Bivalves as indicators of environmental variation and potential anthropogenic impacts in the southern Barents Sea over multiple time scales. Marine Pollution Bulletin 59:193-206. doi:10.1016/j.marpolbul.2009.02.022.

Bivalves as indicators of environmental variation and potential anthropogenic impacts in the southern Barents Sea

Michael L. Carroll[1,*], Beverly J. Johnson[2], Gregory A. Henkes[2,3†],Kelton W. McMahon[4], Andrey Voronkov[5,6], William G. Ambrose, Jr.[1,3], Stanislav G. Denisenko[5]

1) Akvaplan-niva, Polar Environmental Centre, N-9296 Tromsø, Norway
2) Bates College, Department of Geology, Lewiston, Maine 04240, USA
3) Bates College, Department of Biology, Lewiston, Maine 04240, USA
4) Woods Hole Oceanographic Institution, MIT-WHOI Joint Program in Biological Oceanography, Woods Hole, MA 02543-1541 USA
5) Zoological Institute, Russian Academy of Sciences, Universitetskaya nab. 1, St. Petersburg, 199034, Russia
6) Norwegian Polar Institute, Polar Environmental Centre, N-9296 Tromsø, Norway

† Current Address: Smithsonian Institution, Museum Conservation Institute, 4210 Silver Hill Road, MRC 534, Suitland, MD 20746-2863, USA

* Corresponding Author:
M.L. Carroll
Tel: +47 7775 0318
Fax: +47 7775 0301
Email: mc@akvaplan.niva.no

Running Head: Arctic bivalves as indicators of environmental variation

Key Words: Arctic, Barents Sea, benthic community, bivalve growth, climate oscillation, environmental forcing, North Atlantic Oscillation, White Sea, sclerochronology, *Serripes groenlandicus*, shell geochemistry, stable isotopes, trace element ratios

Abstract

Identifying patterns and drivers of natural variability in populations is necessary to gauge potential effects of climatic change and the expected increases in commercial activities in the Arctic on communities and ecosystems. We analyzed growth rates and shell geochemistry of the circumpolar Greenland smooth cockle, *Serripes groenlandicus,* from the southern Barents Sea over almost 70 years between 1882 and 1968. The datasets were calibrated via annually-deposited growth lines, and growth, stable isotope ($\delta^{18}O$, $\delta^{13}C$), and trace elemental (Mg, Sr, Ba, Mn) patterns were linked to environmental variations on weekly to decadal scales. Standardized growth indices revealed an oscillatory growth pattern with a multi-year periodicity, which was inversely related to the North Atlantic Oscillation Index (NAO), and positively related to local river discharge. Up to 60% of the annual variability in the Ba/Ca could be explained by variations in river discharge at the site closest to the rivers, but the relationship disappeared at a more distant location. Patterns of $\delta^{18}O$, $\delta^{13}C$, and Sr/Ca together provide evidence that bivalve growth ceases at elevated temperatures during the fall and recommences at the coldest temperatures in the early spring, with the implication that food, rather than temperature, is the primary driver of bivalve growth. The multi-proxy approach of combining the annually integrated information from the growth results and higher resolution geochemical results yielded a robust interpretation of biophysical coupling in the region over temporal and spatial scales. We thus demonstrate that sclerochronological proxies can be useful retrospective analytical tools for establishing a baseline of ecosystem variability in assessing potential combined impacts of climatic change and increasing commercial activities on Arctic communities.

1. Introduction

The Arctic is warming and consequently becoming more accessible to industrial and commercial activities such as petroleum and mineral extraction, shipping, and fisheries (ACIA, 2005). As these activities increase, pre-industrial baselines of the natural system are necessary in order to assess the effects of anthropogenic activities on the Arctic marine ecosystem. This necessitates observations and data collections over time scales that capture the seasonal to decadal scales of system processes. Unfortunately, due to the remote setting and harsh nature of much of the Arctic marine ecosystem, relevant scales of observation are rarely adequate with traditional marine biological sampling plans, which usually provide a spatially- and temporally-limited view of the system. While continuously-recording observatories are a promising development (e.g. Morison et al., 2002), they are still in their infancy in the Arctic and currently provide data for limited locations. Biological proxies may provide an immediate alternative approach for assessing the variability of marine ecosystems over longer time frames, including the ability for retrospective reconstruction of environmental variability over historical time frames. Marine bivalves (clams) show great promise for investigating environmental variability in the Arctic. Arctic bivalves are long-lived (decades to centuries), sessile, and often dominate the biomass of many Arctic benthic communities (Zenkevich, 1963; McDonald et al., 1981; Dayton, 1990; Feder et al., 1994). Since bivalve growth is strongly regulated by temperature and food availability (Beukema et al., 1985; Jones et al., 1989; Lewis and Cerrato, 1997; Decker and Beukema, 1999), analyzing variations in growth can provide insight into seasonal to decadal variations in these factors over the animal's life.

Reconstructing environmental conditions from animal soft tissues offers a limited view of the past because of the rapid turnover rates of these highly metabolically-active tissues. Aragonitic bivalve shells, however, are secreted sequentially with external growth

lines as the animal grows (Rhoads and Lutz, 1980), recording the growth histories, metabolism and environmental conditions experienced during the deposition of that shell material. The growth and chemistry of accretionary hard-parts precipitated by marine organisms have proved valuable in developing histories of environmental change in marine systems (Pannella, 1971; Andrews, 1972, 1973; Rhoads and Lutz, 1980; Jones, 1981; Weidman et al., 1994; Witbaard et al., 1999; Ambrose et al., 2006; reviewed in Richardson, 2001). High-latitude bivalves have provided uninterrupted long-term records of hydrographic conditions experienced during the lifetime of the organism (Thompson et al., 1980; Witbaard et al., 1999; Dutton et al., 2002; Müller-Lupp and Bauch, 2005).

The shell material of bivalves preserves chemical proxies for ambient seawater conditions when the organism is actively precipitating shell carbonate. Profiles of stable oxygen and carbon isotopes (Jones and Quitmyer, 1996; Klein et al., 1996; Müller-Lupp and Bauch, 2005; Simstich et al., 2005) and incorporated trace elements (Torres et al., 2001; Vander Putten et al., 2000; Khim et al., 2003; Freitas et al., 2006; Gillikin et al., 2006a) from sequential sampling along the shell height can provide high-resolution records of seawater chemistry useful for interpreting spatial and temporal patterns in temperature, salinity, and hydrography. External growth lines on bivalve shells often represent annual growth checks, as has been demonstrated for *Serripes groenlandicus* (Khim, 2002; Khim et al., 2003; Ambrose et al., 2006; Kilada et al., 2007). Provided the date of death is known, growth lines can be used to determine growth rates and assign calendar years to geochemical proxies. The combined use of growth rate and shell geochemistry allows us to compare proxy information on specific environmental parameters and their biological manifestation, thereby allowing broader inferences on mechanistic relationships of bio-physical coupling.

The Barents Sea, a continental shelf sea bounded by Norway and Russia to the south and the Arctic Ocean basin to the north, is both bathymetrically and hydrographically

complex (Loeng, 1991; Vinje and Kvambekk, 1991). The northern and eastern regions are dominated by Arctic water with origins in the Arctic Ocean and Russian shelf seas. The southern region is strongly influenced by warm, saline Atlantic source water from temperate latitudes. The coastal areas of the southern Barents Sea are under the influence of the eastern-flowing Murman Coastal Current as well as freshwater discharges from the Mezen', Severnaya Dvina, and Pechora Rivers (Loeng 1989, 1991; Loeng et al., 1997). These oceanographic regions and their hydrographic properties have strong influences on regional and local primary production and ecosystem structure (Wassmann et al., 2006), including benthic community structure (Carroll et al., 2008a) and functioning (Renaud et al., 2008). The overriding influence of these oceanographic provinces on properties of marine ecosystems is modified by regional climatic drivers which oscillate between different phases and are accompanied by substantially different atmospheric and hydrograhic properties over decadal scales. The North Atlantic Oscillation Index (NAO), usually defined as the atmospheric pressure difference between Iceland and Gibraltar, is one of the major modes of variability in the atmosphere of the Northern Hemisphere, (Jones et al., 1997; Osborn et al., 1999), and has been linked to weather patterns and concomitant ecosystem variability throughout Europe (e.g. Ottersen et. al., 2001).

Bivalve populations exhibit growth rates that vary with water masses in the Barents Sea (Tallqvist and Sundet, 2000; Carroll et al., 2008b, Carroll et al., submitted) and bivalves in the seasonally ice covered northern Barents Sea and Svalbard have been shown to be reflective of both large scale climatic forcing and more localized environmental conditions (Ambrose et al., 2006; Carroll et al., submitted). Climate variability in the Barents Sea has caused decadal-scale changes in the recruitment and productivity of commercially important fisheries and in the diversity and biomass of macrobenthic communities (Blacker, 1957, 1965; Denisenko et al., 1995; Sakshaug, 1997; Ottersen and Stenseth, 2001; Stenseth et al., 2004;

Beuchel et al., 2006; Drinkwater, 2006). Detection of these climatic changes over long time scales is a necessary prerequisite to identifying scales of variability and thus assessing more direct anthropogenic effects related to local commercial activities.

We developed a long-term sclerochronological record of environmental change using the Greenland Smooth Cockle (*Serripes groenlandicus*) as an Arctic biological proxy. To do this, we investigated the variability of growth histories, stable isotopes ($\delta^{18}O$ and $\delta^{13}C$), and trace elements (Mg, Sr, Ba, Mn) in archived *S. groenlandicus* shells from the southern Barents Sea near the entrance to the White Sea collected over a period of almost 70 years. By analyzing interannual patterns of growth and trends in stable isotope and trace element ratios from different time periods, we demonstrate the use of bivalves as proxies leading to a better understanding of the range of variability in these Arctic systems over multiple temporal scales. This information will provide essential information about ecosystem function in this present era of climate change and increasing commercial activities in the Arctic.

2. Materials and Methods

2.1. Sample Collection

The Greenland Smooth Cockle (*Serripes groenlandicus*, hereafter referred to as 'cockles') is a circumpolar bivalve with a maximum size of about 100 mm and age of about 30 years (Kilada et al., 2007). The Laboratory of Marine Research, Zoological Institute of the Russian Academy of Sciences, St. Petersburg (LMR-ZIN) maintains extensive collections of biological materials collected during Russian Arctic expeditions well into the 19th century. We made searches of the LMR-ZIN collections from original hand-written expedition logs of Arctic past expeditions in order to identify samples of cockles from the Barents Sea-Svalbard region. Specimens were then examined to make sure they met criterion making them suitable for analyses in the present project (e.g. precise collection coordinates, the presence of whole animals as well as shells indicating live collection, shells intact).

126 From this visual inspection, roughly 100 individuals were identified as potentially
127 appropriate for use in the project. These individuals were further culled based on the time and
128 location of collection, the size of individuals, and the visibility of growth lines on the shell.
129 This resulted in a final sample population of 15 individuals from the southern Barents Sea in
130 proximity to the entrance to the White Sea (Fig. 1), collected on expeditions between 1899
131 and 1968 (Table 1). These individuals covered the time period between 1882 and 1968,
132 excluding only 1900-1904 and 1928-1943 (Table 1, Fig. 2). Here, we present growth data
133 from all 15 of our shells, and geochemical data from two of the 15 shells.

134 ## *2.2. Growth Rates*

135
136 Each annual increment was measured externally as the linear length from the umbo to
137 each successive dark growth line along the axis of greatest shell height toward the ventral
138 shell margin. Since individuals were collected in the middle of a growth year, the last
139 increment (outermost growth beyond the last dark growth line) was incomplete, and therefore
140 excluded from further analyses. Measurements were made with MapViewer software from
141 high resolution photographs and corroborated with caliper-based measurements of the total
142 shell height. Cockles were collected live, so each growth increment can be assigned to a
143 specific calendar year by counting sequentially back from the year of collection.
144 Bivalve growth declines with age, so raw growth increments within an individual and
145 among individuals of different ages must be standardized before growth can be compared
146 among years. We used the methods of Jones et al. (1989), employing the von Bertalanffy
147 growth function with respect to time, to derive an ontogenetically-adjusted measure of annual
148 growth (see Ambrose et al. (2006) and Carroll et al. (submitted) for a complete description of
149 the application of the von Bertalanffy function to cockle populations).
150 After determining the average yearly changes in shell height based on growth data
151 from all cockles in the sample population, we calculated the expected yearly increase in shell

height for each cockle for each year. We then divided the measured yearly shell growth by the expected growth for that year to generate a Standardized Growth Index (SGI). This removed ontogenetic changes in growth and equalized the variance for the entire growth series (Fritts, 1976). The result is a record of year-by-year growth for the population. An SGI greater than 1.0 indicates a better than expected year of growth, while a value less than 1.0 reflects less than expected growth for that year. The growth rate of individuals at each station was determined by comparing growth curves (age at shell height) for each station. This was done by generating omega (ω) values for each individual at each station. The omega value is a single growth parameter derived from the von Bertalanffy growth function (Jones et al., 1989):

$$\omega = SH_{\infty} * k$$

where SH_{∞} = maximum asymptotic shell height and k = growth constant. This parameter corresponds to the growth rate near t_0 and is suitable for comparisons of organism growth-functions between regions (Gallucci and Quinn, 1979; Appledoorn 1980, 1983; Jones et al., 1989).

2.3. Geochemical Analyses

2.3.1. Sample Preparation

Two archived shells (collection numbers 156 – collected in 1926, and 262 – collected in 1968, Table 1) were selected for analyses of stable oxygen and carbon isotope ratios ($\delta^{18}O$ and $\delta^{13}C$) and trace element ratios (Mg/Ca, Sr/Ca, Ba/Ca, Mn/Ca) based on the condition and thickness of shells and to maximize temporal coverage (Table 2). Both archived specimens remained completely intact (shell and soft tissue) during storage at LMR-ZIN and were preserved in 95% ethanol at room temperature since collection. Ethanol has not been demonstrated to affect shell geochemistry (Xia et al., 1997; Ito, 2001). The shells were rinsed with deionized (DI) water after removal from preservative and air dried prior to sectioning.

178 One valve from each specimen was thinly coated in polyvinyl alcohol and embedded
179 in epoxy (Buehler Ltd., Illinois, USA). Thin sections (2 mm thick) of the shells were cut
180 along the line of maximum growth with a low-speed diamond saw, fixed to petrographic
181 slides with epoxy, rinsed with deionized water, and air-dried. Each thin section was polished
182 on the sample face using 240, 320, 400, 600 grit abrasive carbide discs and a polishing cloth
183 with 0.3 μm Al_2O_3 polishing powder according to Ambrose et al. (2006).

184 ### 2.3.2. Stable Oxygen and Carbon Isotope Analysis
185
186 Shell material for oxygen and carbon stable isotope analyses was milled from thin
187 sections with a rounded 150 μm diameter drill bit on a computer programmed Merchantek
188 Micromill™ at the Micropaleontology Mass Spectrometry Facility (Woods Hole
189 Oceanographic Institution (WHOI), Massachusetts, USA). We milled approximately 5-6
190 individual sample points per growth increment across 14-16 years from each shell (Table 2).
191 We obtained 20-180 μg of carbonate shell material from an individual sample point by
192 drilling 6-8 adjacent target holes (150 μm diameter, 450 μm deep) parallel to the plane of
193 shell growth (Fig. 3). Micro-milling was targeted within the prismatic middle shell layer and
194 within the darker, denser annual growth lines. Material from the nacreous and the organic-
195 rich periostracum, which may be metabolically reworked or susceptible to diagenesis, was
196 avoided. Khim et al. (2003) confirmed, using X-ray diffraction analysis, that prismatic
197 material sampled from *S. groenlandicus* is entirely composed of aragonite.
198 Powdered carbonate shell samples were analyzed for oxygen and carbon stable
199 isotopes with a ThermoFinnigan Kiel III device coupled to a Finnigan MAT252 isotope ratio
200 mass spectrometer (IRMS) at the Micropaleontology Mass Spectrometry Facility (WHOI).
201 Samples were reacted with 100% phosphoric acid at 70ºC to liberate CO_2 inline to the IRMS.
202 The $CaCO_3$-CO_2 fractionation factors of Friedman and O'Neal (1977) were used to calculate
203 the isotopic composition of the carbonate samples. The samples were calibrated against the

204 NBS-19, B1, and AtlantisII standards and all data are reported as permil (‰) VPDB in the
205 conventional δ-notation according to the following definition:

206 $$\delta X\left(‰\right) = \left[\left(\frac{R_{\text{Sample}}}{R_{\text{Standard}}}\right) - 1\right] * 1000$$

207 where *X* is ^{18}O or ^{13}C and R is the ratio of $^{18}O/^{16}O$ or $^{13}C/^{12}C$. Long-term precision estimates
208 of the mass spectrometer based on analyses of NBS-19 are $\delta^{18}O$: ± 0.07 and $\delta^{13}C$: ± 0.03
209 (Ostermann and Curry, 2000).

210 Shell thin sections used for oxygen and carbon stable isotope sampling were post-
211 processed with a Nikon SMZ1500 stereo-microscope and a 2 mega-pixel color camera at the
212 Bates College Imaging and Computing Center (Maine USA) to calibrate individual sampling
213 points to shell length. A composite image of each specimen was created by stitching together
214 20-30 images (56.4 cm × 42.3 cm) using Adobe Photoshop CS3 (Adobe Systems, San Diego,
215 CA).

216 ### 2.3.3. Trace Element Ratio Analysis
217

218 Trace element (Mg, Sr, Ba, Mn, and Ca, the latter used to normalize the other elements)
219 analyses were conducted on shell thin-sections via a New Wave Research UP213 laser
220 ablation system coupled to a ThermoFinnigan Element2 single-collector sector field ICP-MS.
221 Thin-sections were prepared identically to those used for stable oxygen and carbon isotope
222 sampling. Thin-sections were cleaned in a class 100 clean room at the Plasma Mass
223 Spectrometry Facility (WHOI) by scrubbing with a nylon brush, rinsing with 2% HNO_3,
224 sonicating for 5 minutes in ultra-pure H_2O, rinsing with ultra-pure H_2O, and drying for 24
225 hours in a laminar flow clean bench according to Ambrose et al. (2006). Approximately 12-
226 15 laser spots (dwell time 60 sec at 10 Hz, spot size 55 μm, laser output 100% power) were
227 shot per growth year (every 125-520 μm along the shell axis) with the last spot of a year

228 landing on the annual growth line. This sampling scheme achieved sub-monthly to monthly
229 resolution. Certified aragonite reference materials of known trace element composition were
230 run every sixth spot to control for machine drift (Yoshinaga et al., 2000; Sturgeon et al.,
231 2005). Instrument set-up was similar to that of Gunther and Heinrich (1999) as modified by
232 Thorrold et al. (2001). External precisions (relative standard deviations) for the lab standard
233 were as follows: Mg/Ca = 1 %, Sr/Ca = 0.6 %, Ba/Ca = 0.8 %, and Mn/Ca = 0.8 %.
234 The location and temporal signature integration for the stable isotope data and the
235 trace element data were probably not synchronous. The oxygen and carbon isotope data were
236 collected via micromilling multiple tightly grouped spots (Fig. 3), which integrated all of the
237 growth line material, and perhaps some material secreted just prior to the growth line. The
238 trace element data, however, were collected via high precision laser ablation, which resulted
239 in much finer spatial (and temporal) resolution.

240 ## *2.4. Environmental Data*

241
242 Various environmental data sets were referenced for correlation with growth data and
243 geochemical information obtained from *S. groenlandicus.* We examined relationships
244 between cockle growth and the North Atlantic Oscillation Index (NAO). Data for the NAO,
245 using the sea level pressure difference between Gibraltar and Southwest Iceland (Jones et al.,
246 1997; Osborn et al., 1999), were obtained from (http://www.cru.uea.ac.uk/cru/data/nao.htm).
247 We used NAO index data from the winter months (December, January, February, and March),
248 as the signal tends to be stronger in winter, and these months precede the active period of
249 growth.
250 Regional terrestrial freshwater input into the White Sea was estimated based on stream
251 flow data from the Severnaya Dvina and Mezen' Rivers. Data from the Severnaya Dvina
252 spans 1882-1999, and the Mezen' spans 1921-1999. While other rivers also discharge into the
253 northern White Sea, they are much smaller than the Severnaya Dvina or Mezen' and have

data records insufficiently short or sporadic for use in the present study. River discharge data were collected by Roshydromet (Russia) and accessed through R-ArcticNET (v.3.0) (http://www.r-arcticnet.sr.unh.edu/v3.0/index.html). As stream flow is highly seasonal in this region, with a very large proportion of total discharge occurring in a short period in summer, we used flows (m^3 s^{-1}) during the peak month of May, and flows summed for the summer season (May, June, July).

Monthly average water temperatures and salinities were estimated at the sampling sites from a dataset presenting integrated averages from 1898 - 1993 (Matishov et al., 1998). At 50 m water depth, long-term seasonal differences in temperature are between 4 and 6 °C, and seasonal salinity values vary by less than 0.5 PSU.

2.5. Data Treatment and Statistical Analyses

Absolute growth rates (ω parameter derived from the modeled von Bertalanffy growth function) were compared among populations using one-way analysis of variance (ANOVA) following *a priori* diagnostic tests for homogeneity of variance between groups and normal distribution of data. Standard linear regressions were used to assess relationships between SGI, NAO, and river discharge patterns. Student's t-tests were used to determine whether statistically significant differences exist between the ranges of intra- and inter-annual geochemical data. We used Pearson correlations and linear regressions to compare trace elemental ratios and stable isotope profiles within individual shells. Errors are reported as standard deviations unless otherwise stated. Statistical computations were carried out with Microsoft Excel and Statistica (ver. 6).

3. Results

3.1. Sample Population Characteristics

279 We analyzed 15 individual *S. groenlandicus*, collected from 8 different locations and
280 three different time periods: 1899, 1926/1927, and 1968 in the southern Barents Sea near the
281 entrance to the White Sea (Table 1, Fig. 1). The largest individual in our dataset was 67.1
282 mm, with a corresponding age of 16 years, and the average size at age 15 was 54.50 ± 9.64
283 mm for the 1899 collected samples, 47.09 ± 6.26 mm for the 1926/27 collected individuals,
284 and 53.53 ±7.76 mm for the 1968 collected individuals. The age range of 15 samples was 6-
285 22 years old, yielding time series lengths of 17 years for the cockles collected in 1899, 23
286 years for the cockles collected in 1926/27 and 22 years for the cockles collected in 1968. In
287 aggregate, the samples provide a total time series of 62 years over the period 1882-1968.
288 Absolute growth rates (ω) varied between a maximum of 4.83 ± 1.62 in 1968 and a
289 minimum of 3.69 ± 0.52, with an intermediate value of 4.53 ± 0.91 in 1899. These variations
290 in the ω growth parameter were not significantly different (One-way ANOVA: $df_{3,14}$, F =
291 1.45, P > 0.05) between the time periods.

292 ## *3.2. Standardized Growth Index (SGI)*
293
294 The von Bertalanffy model was an excellent descriptor of cockle growth (R^2 = 0.993,
295 P<0.0001). This allowed us to confidently correct for ontogenetic changes in growth with age
296 and thereby compare actual versus the expected growth for each calendar year (SGI).
297 SGI varied considerably over the 17-23 year periods covered by the three time periods
298 (Fig. 4), ranging for individual clams from a low of 0.17, 0.24, and 0.24 in the poorest growth
299 years (1898, 1926, and 1967, respectively) to highs of 2.42, 2.74, and 2.11 in the best growth
300 years (1887, 1918, and 1955, respectively). The mean population SGIs from each time period
301 ranged from lows of 0.79 (1884), 0.50 (1905), and 0.46 (1966) to highs of 1.87 (1891), 1.44
302 (1918), and 1.65 (1955) (Fig. 4). SGI varied both within and among time periods with the
303 highest average value (1.18 ± 0.27) in the 1899 collection and the lowest (0.94 ± 0.25) in the

in1926/27 collection. The 1899 collection had 80% of growth years with SGI over 1.0, compared to 33% for the 1926/27 collection. The SGI pattern in each time period oscillates between higher and lower values over a period of 4-6 years, rather than varying dramatically between single consecutive years (Fig. 4). This serial autocorrelation among years indicates a multi-year periodicity in the growth rates of these bivalves.

3.3. Stable Isotope and Trace Elemental Ratios

3.3.1. Stable Oxygen and Carbon Isotopes

The stable oxygen and carbon isotope profiles of both samples were characterized by seasonal cycles corresponding to the annual growth lines. $\delta^{18}O$ values were fairly uniform for most of the growing season, except for a characteristic strong depletion in ^{18}O at or just before the annual growth line (Fig. 5). The overall mean $\delta^{18}O$ value from shell 156, covering the period 1907-1922, (3.43 ± 0.59 ‰), was significantly lower than shell 262 covering the period 1946-1959, (3.73 ± 0.27 ‰) (Student's t-test, $P < 0.001$). The average $\delta^{18}O$ minima recorded on the growth lines of both shells were significantly more depleted than the average intra-annual $\delta^{18}O$ values (Student's t-tests, $P < 0.001$): 2.99 ± 0.46 ‰ vs. 3.55 ± 0.57 ‰ for 156 and 3.46 ± 0.29 ‰ vs. 3.83 ± 0.17 ‰ for 262. In shell 156, there was a large minimum in $\delta^{18}O$ in 1914, representing an approximate 3.9 ‰ deviation from the cyclic $\delta^{18}O$ pattern.

The carbon stable isotope profiles for both shells covary with the $\delta^{18}O$ profiles (Fig. 5). Similar to the $\delta^{18}O$ profiles, there are significant intra-annual differences in $\delta^{13}C$ values from annual lines and the summer material for shells 156 (Student's t-test, $P = 0.003$) and 262 (Student's t-test, $P < 0.0001$). $\delta^{13}C$ showed characteristic strong depletions in ^{13}C at or just before the annual growth line.

3.3.2. Trace Element Ratios

329 Trace element ratios in shell 156 reflect years 1907-1912 (Fig. 6) and in shell 262
330 reflects years 1957-1962 (Fig. 7). Both shells exhibit annual periodicity for all trace element
331 ratios, corresponding to the annual growth lines on shell cross-sections. Shell 156 showed a
332 consistent seasonal pattern in Sr/Ca and Mg/Ca ratios, where annual minima corresponded to
333 the growth lines, followed by sharp increases in Sr/Ca, and to a lesser extent Mg/Ca,
334 immediately following the growth line, and ending with a gradual decline approaching the
335 next growth line (Fig. 6). This trend was closely mimicked by the Ba/Ca ratios (Sr/Ca: R^2 =
336 0.49, $P < 0.0001$; Mg/Ca: $R^2 = 0.42$, $P < 0.01$) and to a lesser degree by the Mn/Ca ratios
337 (Sr/Ca; $R^2 = 0.16$, $P > 0.05$; Mg/Ca: $R^2 = 0.42$, $P < 0.01$).
338 The trace element profiles for shell 262 exhibit a similar annual cyclicity as shell 156
339 (Fig. 7). Annual minima for Sr/Ca are coincident with growth lines in years 1959, 1961, and
340 1962, however in the other years (and for all years in the Mg/Ca profile) the annual minima
341 appears just before the growth line. In addition, there appears to be a decoupling of Sr/Ca and
342 Mg/Ca ratios for some years that was not seen in shell 156. Ba/Ca and Mn/Ca ratios,
343 however, showed consistent seasonal patterns, with annual minima on the growth lines and
344 maxima in the intra-growth line material. The Ba/Ca and Mn/Ca profiles in shell 262 strongly
345 covary ($R^2 = 0.88$, $P < 0.0001$). The patterns of Ba/Ca and Mn/Ca ratios in shell 262 were
346 similar to those in shell 156. Shell 262 had a significantly lower average Ba/Ca ratio
347 compared shell 156 (Student's t-test, $P = 0.006$).

348 ### *3.4. Environmental Relationships*
349
350 There is an inverse relationship between cockle SGI and NAO that was evident in the
351 combined data from all three time periods (pooled $R^2 = 0.20$, $P < 0.001$), with episodes of
352 positive NAO generally associated with low SGI and vice versa. However, this relationship is
353 inconsistent among time periods (Fig. 8); it is strongest from 1882-1899 ($R^2 = 0.61$, $P <$
354 0.001), relatively weaker from 1904-1927 ($R^2 = 0.35$, $P < 0.01$), and statically insignificant

355 from 1946-1968 (R^2 = 0.15, P = 0.07). The 1899-collected population had the highest overall
356 SGIs, had relatively higher SGI values for a corresponding NAO, and also exhibited the
357 strongest effect of NAO on SGI, indicated by the steeper slope of the relationship. This
358 period was also one in which NAO values consistently negative (i.e. never exceed 1.0); the
359 other time periods all experienced NAO values up to 2.0.
360 One main manifestation of the NAO is precipitation in Northern European areas, which can
361 be reflected in river discharges (e.g. Peterson et al., 2002). In the Arctic, river discharges are
362 strongly seasonal, with the vast majority of flow occurring in the spring and early summer.
363 The Severnaya Dvina is the largest river to discharge into the White Sea, and has a catchment
364 watershed of 348,000 km^2 and an average volume of 105 km^3 yr^{-1} (Peterson et al., 2002).
365 Despite strong interannual variability, summer discharges tended to exhibit multi-annual
366 trends at decadal-scale frequencies (Fig. 9). Discharges generally increased during the life
367 spans of the 1899-collected individuals, were steady or decreased during the life spans of the
368 1926/27 collected individuals, and were quite variable during the life spans of the 1968
369 collected individuals (Fig. 9). There is a positive relationship (R^2 = 0.45) between summer
370 river discharge and SGI (Fig. 10) in the 1899-collected population, with higher SGIs
371 occurring during years of higher summer discharges of the Severnaya Dvina. This relationship
372 is undetectable in the other time periods (R^2 < 0.11, P > 0.05), reflecting the reduced influence
373 of river discharge on SGI at lower discharges.
374 There also appears to be an effect of river discharge on the Ba/Ca ratio in sample shell
375 156 with years of higher discharges of the Severnaya Dvina resulting in higher Ba/Ca ratios in
376 the shells (Fig. 11). Summer river discharges explained 62% of the variation in the Ba/Ca
377 isotope ratios. A similar relationship was found between Ba/Ca ratios in shell 156 and the
378 discharge of the Mezen' River (a smaller river that also empties into the White Sea). The

379 relationship between river discharge and Ba/Ca ratios in sample shell 262, however, was
380 substantially weaker ($R^2 = 0.29$).

381 4. Discussion

382
383 Both growth rates and geochemical proxy data of the *S. groenlandicus* shells spanning
384 from 1882-1968 from the southern Barents Sea exhibited distinct cyclic patterns on different
385 time scales ranging from seasons to decades, reflecting scales of variability in the various
386 components of the physical environment. Growth rates (SGI) exhibited an interannual pattern
387 of variability consistent with large-scale climate regulation through the NAO, as locally
388 modified through interannual variations in river discharge. $\delta^{18}O$ and $\delta^{13}C$ showed
389 characteristic seasonal patterns, the former reflecting variations in local and regional
390 temperature while the latter was linked to hydrographic conditions. Elemental
391 paleothermometers support previous findings that annual growth lines in *S. groenlandicus* are
392 deposited in winter (Ambrose et al., 2006). Meanwhile, Ba/Ca patterns provide a link to the
393 regional influence of river discharge to the coastal hydrography of the southern Barents Sea.

394 *4.1. Growth Rates and Environmental Relationships*

395
396 Overall growth rates among the different times periods were not significantly different
397 despite the fact that they were collected at different times, at different locations within the
398 area (Fig. 1), and at various depths (Table 1). The 1899 collection, in particular, had some
399 samples collected at a much greater depth (190 m) than the other populations (60-70 m). This
400 deeper site was, however, very near the coast and the depth evidently didn't strongly
401 influence the overall growth rates. Thus we presume some intra-regional consistency in the
402 factors affecting growth in these populations.

403 The SGI pattern of relative growth among years exhibited a similar qualitative pattern
404 in each time period, oscillating between higher and lower values over periods of 4-6 years.

405 This serial autocorrelation among years indicates a multi-year periodicity in the growth rates
406 of these bivalves, suggesting a response to an external driver with a similar periodicity. SGI
407 oscillations of this temporal periodicity have been demonstrated for *S. groenlandicus* from
408 northern Svalbard (Ambrose et al., 2006) and another cockle, *Clinocardium ciliatum*, in the
409 northwest Barents Sea (Carroll et al., submitted). Both studies identified relationships with
410 atmospheric large-scale drivers, primarily with the Arctic Climate Regime Index (ACRI), but
411 also with the NAO in Atlantic dominated areas of the Barents Sea. In the present study, we
412 have established an inverse relationship between SGI and the NAO (Fig. 8), which was
413 clearly apparent around the turn of the 20th century, but not detectable in the 1920's or 1960's.
414 The NAO is a well-known driver of atmospheric patterns in the North Atlantic region
415 (Jones et al., 1997; Osborn et al., 1999) that is thought to broadly influence a number of
416 climatic and meteorological patterns from the northeast coast of North America through
417 Europe and the Mediterranean region. There is widespread evidence of the influence of the
418 NAO on ecological components in both the terrestrial and marine ecosystems in the North
419 Atlantic region (Ottersen et al., 2001), including phytoplankton, zooplankton, fish, and birds
420 (Reid et al., 1998; Beaugrand et al., 2002; Durant et al., 2004; Richardson and Schoeman,
421 2004; Hátún et al., 2005; Heath, 2005; Perry et al., 2005; Hansen and Samuelsen, submitted).
422 The bivalve, *Arctica islandica,* from North and Norwegian seas has been found to respond to
423 the NAO (Schöne et al., 2005), and marine benthic species diversity and abundance patterns
424 in Kongsfjorden (western Svalbard) exhibited strong shifts coincident with phase shifts in the
425 NAO (Beuchel et al., 2006).
426 The relationship between cockles' SGI and NAO in the southern Barents Sea is
427 apparently manifested locally through variations in discharges of the major rivers emptying
428 into the White Sea: the Severnaya Dvina and, to a lesser extent the Mezen'. Flows of these
429 rivers are strongly seasonal, with the vast majority of discharges occurring during a small

window from May to July (Lammers et al., 2001; Ye et al., 2004). There is also strong interannual variation in river flows (Fig. 9) that is inversely related to the NAO ($R^2 = 0.42$). Further, both SGI (Fig. 10) and the Ba/Ca ratio (Fig. 11, discussed further below) are related to variations in river discharges. Large volumes of freshwater discharged episodically from rivers into the coastal oceans in the Arctic can affect myriad properties of seawater (Peterson et al., 2002; Ye et al., 2004; Milliman and Syvitski, 2002) and serve as a conduit for environmental contaminants to coastal oceans (AMAP, 1998; MacDonald et al., 2000; J. Carroll et al., 2008). Large seasonal river plumes in the Arctic can detrimentally affect marine primary producers in their immediate vicinity and reduce the diversity and biomass of benthic communities through light attenuation, osmotic stress, and smothering (e.g. Dahle et al., 1998, Denisenko et al., 2003). Beyond the plume, however, rivers can stimulate primary and secondary production by delivering large loads of organic carbon and nutrients as food sources for coastal marine communities and stabilizing the water column leading to spring blooms (Opsahl et al., 1999; Dittmar and Kattner, 2003; Stein et al., 2003). Although we have no specific information from the sites on interannual variations in primary production, the relationship between SGI and river discharge suggests that, at least in periods of high flows, the rivers are mediating the SGI patterns in the coastal sea.

It is somewhat curious that the greatest river discharges from the Severnaya Dvina occurred during the periods of NAO in the negative phase, because it is generally acknowledged that a positive NAO will drive a storm track leading to greater precipitation in the northern parts of Europe, with relatively drier conditions over the Mediterranean Region. There are, however, strong intra-regional differences in the strength of the NAO in northern Europe. For example, Uvo (2003) demonstrated that the NAO negative storm track leads to a disproportionately heavy precipitation in the coastal regions and mountains of western Norway but far less precipitation in the leeward locations in northern Scandinavia. We

455 postulate that this intra-regional variation leads to greater river discharges, and associated
456 higher SGIs (Fig. 10) during the negative phase of the NAO in our study region.

457 *4.2. Stable Isotopes*

458
459 We found cyclical patterns in shell $\delta^{18}O$ and $\delta^{13}C$ profiles centered around external
460 growth lines (Fig. 5), which supports findings from previous research with a number of
461 bivalve species (Khim et al., 2003; Simstich et al., 2005; Ambrose et al., 2006). $\delta^{18}O$ values
462 fluctuated seasonally with patterns that were generally consistent among years for both shell
463 156 and 262 (Fig. 5), and were typically most depleted in ^{18}O at or just before the annual
464 growth line. Such patterns in *S. groenlandicus* have been measured elsewhere, and are
465 attributed to rapid cessation of growth immediately after maximum temperatures are reached
466 (Khim et al., 2003).

467 The depletion in $\delta^{18}O$ values at or just before the winter growth line likely results
468 from the combined influenced of higher water temperatures at this time of year. Using the
469 temperature fractionation model of -0.23 ‰ $°C^{-1}$ (Grossman and Ku, 1986), and an average
470 seasonal difference in $\delta^{18}O$ values of 0.63 ‰ in shell 156 and 0.37 ‰ in shell 262, the
471 temperature proxy-calculated seasonal temperature change is 2.8-1.6 °C, and accounts for a
472 substantial portion of the magnitude of the measured ~5°C seasonal range at the sampling
473 sites (Matishov et al., 1998). Seasonal changes in water salinity occur after the spring melt
474 and may also influence the $\delta^{18}O$ pattern. Although seasonal variations in salinity in these
475 locations are less than 0.5 PSU at 50 m depth (Matishov et al., 1998), small change can have
476 substantial influences in $\delta^{18}O$. With measured $\delta^{18}O$ values of freshwater in the White Sea of -
477 15.5 ‰ (Nikolayev and Nikolayev 1988) and an estimated full ocean salinity endpoint of 0
478 ‰, a linear regression estimates a change of 0.44 ‰ PSU^{-1}. The resulting 0.22 ‰ range over

479 the measured change of 0.5 PSU at the study sites can thus account for 35-59 % of the
480 average seasonal range in $\delta^{18}O$ in addition to the temperature effect.

481 It is important to note that bivalve shells cannot provide a full record of the annual
482 temperature range because the shells only record ambient environmental conditions during
483 active growth. Thus the oxygen isotope- and mineral-derived temperature records from shell
484 carbonate in organisms that experience dormancy are by definition truncated during dormancy
485 (Schöne 2008).

486 Ecological dormancy in the Arctic winter is thought to result from a combination of
487 extremely low temperatures and lack of food supply (e.g. Falk-Petersen et al., 2000; but see
488 Buick and Ivany, 2004). In fact, food supply and temperature do not vary synchronously. The
489 spring bloom results in an ample food supply to consumers in the Arctic spring when
490 temperatures are at their lowest, and conversely, late fall in the Arctic (i.e. September-
491 October), is a period of high water temperature yet little food availability. Seasonal patterns
492 of food availability, as opposed to temperature, can be the primary driver of bivalve growth
493 (Nakaoka, 1992; Nakaoka and Matsui, 1994). Evidence from the Barents region suggests that
494 *S. groenlandicus* and *C. ciliatum* in the ice covered waters of the northwest Barents Sea and
495 western Svalbard cease growth in late fall due to limited food availability despite warm water
496 temperatures, and then resume growth immediately after fresh food reaches the bottom,
497 despite water temperatures being at their coldest (Carroll et al., submitted). We suggest that
498 the oxygen stable isotope data from the annual growth lines reflect this period of warm
499 ambient water temperatures and food limitation as the as the cockle prepares for dormancy.

500 Shell 156 showed larger intra-annual variations in $\delta^{18}O$, was significantly lighter on
501 average (by 0.3 ‰), and exhibited higher average Ba/Ca values compared to shell 262. These
502 geochemical differences between shells may reflect differences in their relative proximity to
503 the sources of river discharge. Shell 156 was located 150 km closer to the two main

freshwater sources to the White Sea, and may reflect a more ^{18}O depleted signal overall and greater seasonality associated with increased seasonal freshwater input from the Severnaya and Mezen' Rivers as compared to shell 262. Such spatial variability thus makes it difficult to attribute differences in $\delta^{18}O$ values between the shells to either temperature or salinity differences alone.

$\delta^{13}C$ covaries with $\delta^{18}O$ on seasonal time scales and reflects contributions of metabolic carbon as well as ambient water DIC (McConnaughey et al., 1997; Lorrain et al., 2004; Gillikin et al., 2006b; McConnaughey and Gillikin, 2008). Shell $\delta^{13}C$ values were typically lowest at or just before the annual growth line (Fig. 5). An increase in metabolic rate coincident with the rapid increase in ambient water temperatures during the fall could increase the relative contribution of ^{13}C-depeleted respired CO_2 to shell carbon resulting in a depleted bulk shell $\delta^{13}C$ value. Additionally, isotopically depleted DIC corresponding to periods of low primary productivity may be incorporated directly into the shell material just before the annual growth line. While metabolic rate and local DIC $\delta^{13}C$ values most likely play the predominant role in determining shell carbon isotope values, seasonal variability in food source and $\delta^{13}C$ (McMahon et al., 2006; Søreide et al., 2006) may also contribute to shell $\delta^{13}C$ values (Michner et al., 1994; Dettman et al., 1999). These explanations are not mutually exclusive and illustrate that more research is need to fully understand the relative importance of metabolic carbon and DIC to shell $\delta^{13}C$, as has been done for other accretionary carbonate structures such as fish otoliths (Thorrold et al., 1997; Solomon et al., 2006).

4.3. Trace Elemental Ratios

Trace element profiles show strong seasonal cycles, much like the stable isotope values, for both shells 156 and 262 (Figs. 5, 6). Sr/Ca and to a lesser extent Mg/Ca exhibited

529 annual minima coincident with the annual growth line, supporting previous research
530 indicating that growth lines are deposited in winter when ambient temperatures are coldest
531 (Ambrose et al., 2006). However, the Sr/Ca and Mg/Ca ratios increased significantly in early
532 spring, contrary to typical profiles for other bivalve species (Stecher et al., 1996; Vander
533 Putten, 2000; Gillikin et al,. 2005; Freitas et al., 2006), suggesting abrupt changes in internal
534 physiology and/or local environmental conditions. Calibration studies indicate that Sr/Ca
535 may be related to growth rate for some bivalve species (Gillikin et al., 2005). The significant
536 increase in Sr/Ca and Mg/Ca ratios between winter and spring may reflect an increase in trace
537 element incorporation due to elevated growth rates in early spring. These abrupt profiles are
538 not expected if the bivalve was continuously recording temperature throughout the year,
539 suggesting internal physiology may confound records of ambient water trace element
540 concentrations during periods of limited growth (Stecher et al., 1996; Schöne, 2008).
541 The annual shell Ba/Ca profiles for *S. groenlandicus* exhibit clear annual periodicity
542 with maximum values occurring early in the growth year (Figs. 5, 6). Such patterns are
543 consistent with both the increase in primary production associated with the spring bloom and
544 freshwater inputs during spring. Bioavailable barium for incorporation into bivalve shells
545 typically comes from two environmental pools: food and water (Stecher et al., 1996; Gillikin
546 et al., 2006a). Some research suggests that barium ingestion, as barite, following diatom
547 blooms may play a role in bivalve shell Ba/Ca ratios (Stecher et al., 1996), while others
548 (Gillikin et al., 2006a) suggest that background Ba/Ca ratios in bivalves are a more reliable
549 proxy for ambient water Ba/Ca ratios. Gilliken et al. (2008) acknowledge that periodic spikes
550 in Ba/Ca are under exogenous environmental control, but can not identify a satisfactory
551 mechanistic explanation. In our bivalves, we saw a strong relationship between May
552 discharge of the Severnaya Dvina River and maximum annual Ba/Ca in shell 156 (Fig. 11).
553 Whether the increase in Ba/Ca ratios in our data are due to increases in ambient water Ba

554 concentration associated with riverine discharge or increases in barium incorporation into
555 organic matter during spring phytoplankton blooms, it is clear that spring freshwater influx
556 was recorded in the Ba/Ca ratios of local bivalves. A similar trend was not found in shell 262,
557 most likely due to the fact that it was located farther from the river influence. The exact
558 mechanism for barium incorporation into mollusk shells is not well understood (Gilliken et
559 al., 2008), and more research needs to be conducted on the relative importance of dietary
560 versus ambient water Ba inputs to bivalve shell Ba/Ca ratios.

561 The Mn/Ca profiles show similar annual cyclicity to Ba/Ca (Figs. 5, 6). Maximum
562 values occur following the deposition of the winter growth check suggesting that elevated
563 Mn/Ca may coincide with blooms in primary productivity in spring. Vander Putten et al.
564 (2000) found similar patterns from Mn/Ca shell profiles and imply that they coincide with
565 Chlorophyll-a peaks (as many as two per year). It is also apparent that particularly Mn/Ca,
566 but also Ba/Ca, exhibit a distinct interannual pattern of decreasing peak values over the 5 year
567 period (1907-1912) covered by the profile (Fig. 6). This proxy evidence suggests a consistent
568 trend of decreasing primary production (Mn proxy) and/or river discharge (Ba proxy) over
569 this period, which is supported by the measured river discharges (Fig. 9).

570 ## *4.4. Summary and Conclusions*

571
572 One of the great advantages of biomonitors such as clam shells is that they provide a
573 relatively uninterrupted record of biological (i.e., growth) and physical conditions while the
574 animal was alive. Their utility, however, hinges upon our ability to decipher the
575 environmental records stored in the shells in light of known ecology and physiology of the
576 organism (Schöne et al., 2008). In our study, we combined growth and geochemical
577 information from cockles collected live at different times in order to produce a
578 sclerochronological record covering time periods substantially greater than the lifespan of an
579 individual cockle.

580 Growth rate variations (via SGI data) indicate a periodicity consistent with an
581 overriding influence of the NAO. The mechanism by which the NAO influence is manifested
582 in growth is via food availability, and the geochemical evidence suggests that variations in
583 river discharge and proximity to the rivers of the White Sea are major determinants of food
584 availability to the benthos of this region.

585 The growth and geochemical evidence address different, but complimentary, temporal
586 and spatial scales. While scleorchronology can identify growth lines at sub-annual resolution
587 (e.g. Schöne et al., 2002; 2004), the SGI results from external growth lines provides an
588 annually and regionally integrated view, filtering out small scale variations into an overall
589 average of yearly and regional conditions. The geochemical results, in contrast, provide much
590 higher resolution temporal and spatial scale information and can be specifically calibrated to
591 local environmental conditions. But these geochemical results cannot independently indicate
592 how such variations will translate into a better or poorer growth year. By relating results of
593 growth and shell geochemistry to local environmental conditions, particularly river
594 discharges, over several decades, and linking these to a plausible external driver, namely the
595 NAO, we provide a mechanistic explanation for strong physical-biological coupling in the
596 southern Barents Sea, particularly during periods of high river discharge. We thus
597 demonstrate the multi-proxy approach of combining the growth and geochemical results as a
598 powerful tool in establishing baselines of ecosystem variability for assessing potential
599 combined impacts of climatic change and increasing commercial activities in this region.

600 # 5. Acknowledgements

601
602 We gratefully acknowledge past financial support from Norsk Hydro, and continuing
603 financial support from StatoilHydro, the Norwegian Research Council, and the Howard
604 Hughes Medical Institute through Bates College. The Laboratory of Marine Research,
605 Zoological Institute of the Russian Academy of Sciences graciously made available extensive

collections of archived material, and thereby opening a window into the fascinating history of early 20th century Arctic expeditions. J. Edgerly assisted in the laboratory at Bates College and the derivation of the SGI data, the Bates College Imaging Center provided advanced photographic and imaging facilities, and V. Savinov produced the map. We also thank S. Thorrold for making laboratory facilities available at WHOI and for valuable discussions, and S. Birdwhistell and D. Ostermann for help with the stable isotope and trace element sampling. This manuscript has been greatly improved following comments by D. Gilliken and an anonymous reviewer. This publication was made possible, in part, by NIH Grant Number P20 RR-016463 from the INBRE Program of the National Center for Research Resources. Its contents are solely the responsibility of the authors and do not necessarily represent the official views of NIH.

6. References

ACIA. 2005. Impacts of a warming arctic: Arctic climate impact assessment. Cambridge University Press, Cambridge, UK.

AMAP. 1998. Assessment Reports: Arctic Pollution Issues. Arctic Monitoring and Assessment Programme, Oslo, Norway 859 pp.

Ambrose Jr., W.G., Carroll, M.L., Greenacre, M., Thorrold, S. & McMahon, K. 2006. Variation in *Serripes groenlandicus* (Bivalvia) growth in a Norwegian high-Arctic fjord: Evidence for local- and large-scale climatic forcing. Global Change Biology 12, 1595-1607.

Andrews, J.T. 1972. Recent and fossil growth rates of marine bivalves, Canadian Arctic, and Late-Quaternary arctic Marine environments. Paleogeography, Paleoclimatology, Paleoecology 11, 157-176.

Andrews, J.D. 1973. Effects of tropical storm Agnes on epifaunal invertebrates in Virginia estuaries. Chesapeake Science 14, 223-234.

Appledoorn, R.S. 1980. The growth and life-history strategy of the soft-shell clam, *Mya arenaria* L. Ph.D. thesis, University of Rhode Island, Kingston, Rhode Island USA.

634 Appledoorn, R.S. 1983. Variation in the growth rate of *Mya arenaria* and its relationship to
635 the environment as analyzed through principal components analysis and the ω
636 parameter of the von Bertalanffy equation. Fisheries Bulletin of the U.S. 81, 75-84.

637 Beaugrand, G., Reid, P.C., Ibañez, F., Lindley, J.A. & Edwards, M. 2002. Reorganization of
638 North Atlantic marine copepod biodiversity and climate. Science 296, 1692-1694.

639 Beuchel, F., Gulliksen, B. & Carroll, M.L. 2006. Long-term patterns of rocky bottom
640 macrobenthic community structure in an Arctic fjord (Kongsfjorden, Svalbard) in
641 relation to climate variability (1980-2003). Journal of Marine Systems 63, 35-48.

642 Beukema, J.J., Knoll, E. & Cadée, G.C. 1985. Effects of temperature on the length of the
643 annual growing season of the Tellinid bivalve *Macoma balthica* (L.) living on tidal
644 flats in the Dutch Wadden Sea. Journal of Experimental Marine Biology and Ecology
645 90, 129-144.

646 Blacker, R.W. 1957. Benthic animals as indicators of hydrographic conditions and climatic
647 change in Svalbard waters. Fisheries Investigations Series 2, 1-59.

648 Blacker, R.W. 1965. Recent changes in the benthos of the West Spitzbergen fishing grounds.
649 International Commission for Northwest Atlantic Fisheries, Special Publication 6,
650 791-794.

651 Buick, D.V & Ivany, L.C. 2004. 100 years in the dark: Extreme longevity of Eocene bivalves
652 from Antarctica. Geology 32, 921-924.

653 Carré, M., Bentlab, I., Bruguier, O., Ordinola, E., Barrett, N.T. & Fontugne, M. 2006.
654 Calcification rate influence on trace element concentrations in aragonitic bivalve
655 shells: Evidences and mechanisms. Geochimica et Cosmochimica Acta 70, 4906-
656 4920.

657 Carroll, J., Savinov, V., Savinova, T., Dahle, S., McCrea, R. & Muir, D.C.G. 2008. PCBs,
658 PBDEs and pesticides released to the Arctic Ocean by the Russian Rivers Ob and
659 Yenisei. Environmental Science and Technology 42, 69-74.

660 Carroll, M.L., Denisenko, S.G., Renaud, P.E. & Ambrose Jr., W.G. 2008a. Benthic infauna of
661 the seasonally ice-covered western Barents Sea: Patterns and relationships to
662 environmental forcing. Deep Sea Research II 55, 2340-2351,
663 doi:10.1016/j.dsr2.2008.05.022

664 Carroll, M.L., Denisenko, S.G., Voronkov, A., Ambrose Jr., W.G., Henkes, G.A., Bosheim,
665 S., Fredheim, B. & Gulbrandsen, T.R. 2008b. Arctic bivalves as indicators of

666 environmental variation. Proceedings of the SPE 9th International Conference on
667 Health Safety and Environment. 15-17 April 2008, Nice, France. SPE111-558.

668 Carroll, M.L., Ambrose Jr., W.G., Levin, B.S., Ratner, A.R., Ryan, S.K.& Henkes, G.A.
669 Climatic Regulation of *Clinocardium ciliatum* (bivalvia) growth in the northwestern
670 Barents Sea. Journal of Marine Systems (submitted).

671 Dayton, P.K. 1990. Polar benthos. In: W.O. Smith (ed.), Polar Oceanography, Part B
672 Chemistry, Biology, and Geology, pp. 631-685. Academic Press, San Diego.

673 Dahle, S., Denisenko, S.D., Denisenko, N.V. & Cochrane, S.J. 1998. Benthic fauna in the
674 Pechora Sea. Sarsia 83, 183-210.

675 Dekker, R. & Beukema, J. 1999. Relations of summer and winter temperatures with dynamics
676 and growth of two bivalves, *Tellina tenuis* and *Abra tenuis*, on the northern edge of
677 their intertidal distribution. Journal of Sea Research 42, 207-220.

678 Denisenko, S.G., Denisenko, S.V. & Dahle, S. 1995. Baseline Russian investigations of the
679 bottom fauna in the southeastern part of the Barents Sea. In: H.R. Skjoldal, C.
680 Hopkins, K.E. Erikstad, H.P., Leinaas, (eds.), Ecology of Fjords and Coastal Waters,
681 pp. 293-302. Elsevier Science, Amsterdam.

682 Denisenko, S.G., Denisenko, N.V., Lehtonen, K.K., Andersin, A.-B. & Laine, A.O. 2003.
683 Macro-zoobenthos of the Pechora Sea (southeastern Barents Sea): Community
684 structure and spatial distribution in relation to environmental conditions. Marine
685 Ecology Progress Series 258, 109-123.

686 Dettman, D.L., Reische, A.K. & Lohmann K.C. 1999. Controls on the stable isotope
687 composition of seasonal growth bands in aragonitic fresh-water bivalves (unionidae).
688 Geochimica et Cosmochimica Acta 63, 1049-1057.

689 Dittmar, T. & Kattner, G. 2003. The biogeochemistry of the river and shelf ecosystem of the
690 Arctic Ocean: a review. Marine Chemistry 83, 103-120.

691 Drinkwater, K. 2006. The regime shift of the 1920s and 1930s in the North Atlantic.
692 Progress in Oceanography 68, 134-151.

693 Durant, J.M., Anker-Nielssen, T., Hjermann, D.Ø. & Stenseth, N.C. 2004. Regime Shifts in
694 the breeding of an Atlantic puffin population. Ecology Letters 7, 388-394.

695 Dutton, A.L., Lohmann, K.C. & Zinsmeister, W.J. 2002. Stable isotope and minor element
696 proxies for Eocene climate of Seymour Island, Antarctica. Paleoceanography 17(2),
697 doi: 10.1029/2000PA000593.

698 Falk-Peteren, S., Hop, H., Budgell, W.P., Hegseth, E.N., Korsnes, R., Lovyning, T.B.,
699 Orbaek, J.B., Kawamura, T. & Shirasawa, K. 2000. Physical and ecological processes
700 in the marginal ice zone of the northern Barents Sea during the summer melt period.
701 Journal of Marine Systems 27: 131-159.

702 Feder, H.M., Naidu, A.S., Jewett, S.W., Hameedi, J.M., Johnson, W.R. & Whitledge, T.E.
703 1994. The northeastern Chukchi Sea: benthos-environmental interactions. Marine
704 Ecology Progress Series 111, 171-190.

705 Freitas, P.S., Clarke, L.J., Kennedy, H., Richardson, C.A. & Abrantes, F. 2006.
706 Environmental and biological controls on elemental (Mg/Ca, Sr/Ca and Mn/Ca) ratios
707 in shells of the king scallop *Pecten maximus*. Geochimica et Cosmochimica Acta 70,
708 5119-5133.

709 Friedman, I. & O'Neal, J.R. 1977. Compilation of stable fractionation factors of geochemical
710 interest. In: M. Fleischer (ed.), Data of Geochemistry, U.S. Geological Survey
711 Professional Paper 440-KK, 6th Ed., Reston, Virginia, USA.

712 Fritts, H.C. 1976. Tree Rings and Climate. Academic Press, New York, 567 pp.

713 Gallucci, V.E. & Quinn II, Z.J. 1979. Reparameterizing, fitting, and testing a simple growth
714 model. Transactions of the American Fisheries Society 108,14-25.

715 Gillikin, D.P., Lorrain, A., Navez, J., Taylor, J.W., Andre, L., Keppens, E., Baeyens, W. &
716 Dehairs, F. 2005. Strong biological controls on Sr/Ca ratios in aragonitic marine
717 bivalve shells. Geochemistry, Geophysics, Geosystems 6, Q05009, doi:
718 10.1029/2004GC000874.

719 Gillikin, D.P., Dehairs, F., Lorrain, A., Steenmans, D., Baeyens, W. & Andre, L. 2006a.
720 Barium uptake into the shells of the common mussel (*Mytilus edulis*) and the potential
721 for estuarine paleo-chemistry reconstruction. Geochimica et Cosmochimica Acta 70,
722 395-407.

723 Gillikin, D.P., Lorrain, A., Bouillon, S., Willenz, P. & Dehairs, F. 2006b. Shell carbon
724 isotopic composition of Mytilus edulis shells: relation to metabolism, salinity, $\delta^{13}C_{DIC}$
725 and phytoplankton. Organic Geochemistry 37, 1371–1382.

726 Gillikin, D.P., Lorrain, A., Paulet, Y.-M., André, L. & Dehairs, F. 2008. Synchronous barium
727 peaks in high-resolution profiles of calcite and aragonite marine bivalve shells. Geo-
728 Marine Letters 28, 351-358. doi: 10.1007/s00367-008-0111-9.

729 Grossman, E.L. & Ku, T.-L. 1986. Carbon and oxygen isotopic fractionation in biogenic
730 aragonite: Temperature effects. Chemical Geology 59, 59-74.

731 Gunther, D. & Heinrich, C.A. 1999. Enhanced sensitivity in laser ablation-ICP mass
732 spectrometry using helium-argon mixtures as aerosol carrier. Journal of Analytical
733 Atomic Spectrometry 14, 1363–1368.

734 Hansen, C. & Samuelsen, A. Interannual variability of the primary production in the
735 Norwegian Sea: relation to the NAO in a numerical model. Marine Ecology Progress
736 Series (submitted).

737 Hátún, H., Sandø, A.B., Drange, H., Hansen, B. & Valdimarsson, H. 2005. Influence of the
738 Antlatic Subpolar Gyre on the Thermohaline Circulation. Science 309, 1841-1844.

739 Heath, M.R. 2005. Changes in the structure and function of the North Sea fish foodweb,
740 1973-2000, and impacts of fishing and climate. ICES Journal of Marine Science 62,
741 405-411.

742 Ito, E. 2001. Application of stable isotope techniques to inorganic and biogenic carbonates.
743 In: W.M Last & J.P. Smol (eds.) Tracking Environmental Change Using Lake
744 Sediments. Springer Netherlands, 351-371

745 Jones, D.S. 1981. Annual growth increments in shells of *Spisula solidissima* recorded marine
746 temperature variability. Science 211, 165-165.

747 Jones, D.S. & Quitmyer, I.R. 1996. Marking time with bivalve shells: Oxygen isotopes and
748 season of annual increment formation. Palaios 11,340-346.

749 Jones, D.S., Arthus, M.A. & Allard, D.J. 1989. Sclerochronological records of temperature
750 and growth from shells of *Mercenaria mercenaria* from Narragansett Bay, Rhode
751 Island. Marine Biology 102, 225-234.

752 Jones, P.D., Jonsson, T. & Wheeler, D. 1997. Extension to the North Atlantic Oscillation
753 using early instrumental pressure observations from Gibraltar and South-West
754 Iceland. International Journal Climatology 17, 1433-1450.

755 Khim, B.K., Krantz, D.E. & Brigham-Grette, J. 2001. Stable isotope profiles of Last
756 Interglacial (Pelukian Transgression) mollusks and paleoclimate implications in the
757 Bering Strait Region. Quaternary Science Reviews 20, 463-483.

758 Khim, B.K. 2002. Stable isotope profiles of Serripes groenlandicus shells. I. Seasonal and
759 interannual variations of Alaskan Coastal Water in the Bering and Chukchi Seas.
760 Geosciences Journal 6, 257-267.

761 Khim, B.K., Kranz, D.E., Cooper, L.W. & Grebmeier. J.M. 2003. Seasonal discharge to the
762 western Chukchi Sea shelf identified in stable isotope profiles of mollusk shells.
763 Journal of Geophysical Research 108 (C9), 3300, doi:10.1029/2003JC001816

764 Kilada, R.W., Roddick, D. & Mombourquette, K. 2007. Age determination, validation,
765 growth and minimum size of sexual maturity of the Greenland Smoothcockle
766 (*Serripes groenlandicus*, Bruguiere, 1789) in Eastern Canada. Journal of Shellfish
767 Research 26(2), 443-450.

768 Klein, R.T., Lohmann, K.C. & Thayer, C.W. 1996. Bivalve skeletons record sea-surface
769 temperature and $\delta^{18}O$ via Mg/Ca and $^{18}O/^{16}O$ ratios. Geology 24, 415-418.

770 Lammers, R.B., Shiklomanov, A. I., Vörösmarty, C.J., Fekete, B.M. & Peterson, B.J. 2001.
771 Assessment of contemporary Arctic river runoff based on observational discharge
772 records. Journal of Geophysical Research 106(D4), 3321–3334.

773 Lewis, D.E. & Cerrato, R.M. 1997. Growth uncoupling and the relationship between shell
774 growth and metabolism in the soft shell clam *Mya arenaria*. Marine Ecology Progress
775 Series 158, 177-189.

776 Loeng, H. 1989. Ecological features of the Barents Sea. In: Rey, L., Alexander, V. (eds.),
777 Proceedings of the 6th International Conference Committee on the Arctic, pp. 327-365.

778 Loeng, H. 1991. Features of the physical oceanographic conditions in the Barents Sea. Polar
779 Research 10, 5-18.

780 Loeng, H., Ozhigin, V. & Ådlandsvik, B. 1997. Water fluxes through the Barents Sea. ICES
781 Journal of Marine Science 54, 310-317. doi:10.1006/jmsc.1996.0165

782 Lorrain, A., Paulet, Y-M., Chauvaud, L., Dunbar, R., Mucciarone, D. & Fontugne, M. 2004
783 $\delta^{13}C$ variation in scallop shells: increasing metabolic carbon contribution with body
784 size? Geochimica et Cosmochimica Acta 68, 3509–3519.

785 Macdonald, R.W., Barrie, L.A., Bidleman, T.F., Diamond, M.L., Gregor, D.J., Semkin, R.G.,
786 Strachan, W.M.J., Li, Y.F., Wania, F., Alaee, M., Alexeeva, L.B., Backus, S.M.,
787 Bailey, R., Bewers, J.M., Gobeil, C., Halsall, C.J., Harner, T., Hoff, J.T., Jantunen,
788 L.M.M., Lockhart, W.L., Mackay, D., Muir, D.C.G., Pudykiewicz, J., Reimer, K.J.,
789 Smith, J.N., Stern, G.A., Schroeder, W.H., Wagemann, R. & Yunker, M.B. 2000.
790 Contaminants in the Canadian Arctic: 5 years of progress in understanding sources,
791 occurrence and pathways. Science of the Total Environment 254, 93-234.

792 Matishov, G., Zyev, A., Golubev, V., Slobodkin, V., Levitus, S. & Smolyar, I. 1998. Climatic
793 Atlas of the Barents Sea 1998: Temperature, salinity, oxygen. World Data Center – A
794 for Oceanography, International Ocean Atlas Series, Volume 1. NOAA Atlas
795 NESDIS 26. Digital Media; also online at:
796 http://www.nodc.noaa.gov/OC5/barsea/barindex1.html.

797 McConnaughey, T.A., Burdett, J., Whelan, J.F. & Paull, C.K. 1997. Carbon isotopes in
798 biological carbonates: Respiration and photosynthesis. Geochimica et Cosmochimica
799 Acta 61, 611-622.

800 McConnaughey, T.A. & Gillikin, D.P. 2008. Carbon isotopes in mollusk shell carbonates.
801 Geo-Marine Letters 28, 287-299.

802 McDonald, J., Feder, H.M. & Hoberg, M. 1981. Bivalve mollusks of the Southeastern Bering
803 Sea. In: D.W. Hood, J.A. Calder (eds.), The Eastern Bering Sea Shelf: Oceanography
804 and Resources, pp. 1155-1204. University of Washington Press, Seattle.

805 McMahon, K.W., Ambrose Jr., W.G., Johnson, B.J., Sun, M.-Y., Lopez, G.R., Clough, L.M.
806 & Carroll, M.L. 2006. Benthic community response to ice algae and phytoplankton in
807 Ny Ålesund, Svalbard. Marine Ecology Progress Series 310, 1-14.

808 Michener, R.H. & Shell, D.M. 1994. Stable isotope ratios as tracers in marine aquatic food
809 webs. In: K. Lajtha, R.H. Michener (eds.), Stable Isotopes in Ecology and
810 Environmental Studies pp. 138–157. Blackwell Scientific Publications,

811 Milliman, J.D. & Syvitski, J.P.M. 1992. Geomorphic/tectonic control of sediment discharge
812 to the oceans: The importance of small mountainous rivers. Journal of Geology 100,
813 525-544.

814 Morison, J.H., Aagaard, K., Falkner, K.K., Hatakeyama, K. Moritz, R. Overland, J.E.,
815 Perovich, D. Shmada, K. Steele, M. Takizawa, T., & Woodgate, R. 2002. North Pole
816 Environmental Observatory delivers early results. Eos 83, 360-361.

817 Müller-Lupp, T. & Bauch, H.A. 2005. Linkage of Artic shelf atmospheric circulation and
818 Siberian shelf hydrography: a proxy validation using δ18O records of bivalve shells.
819 Global Planetary Change 48,175-186.

820 Nakaoka, M. 1992. Spatial and seasonal variation in growth rate and secondary production of
821 *Yoldia notabilis* in Otsuchi Bay, Japan, with reference to the influence of food supply
822 from the water column. Marine Ecology Progress Series 88, 215–223.

823 Nakaoka, M. & Matsui, S. 1994 Annual variation in the growth rate of *Yoldia notabilis*
824 (Bivalvia: Nuculanidae) in Otsuchi Bay northeastern Japan analyzed using shell
825 microgrowth patterns. Marine Biology 119, 397-404.

826 Nikolayev, V.I & Nikolayev, S.D. 1988. Formation of the oxygen isotopic composition of
827 waters of the White Sea Basin, Water Resources 14, 408-411.

828 Osborn, T.J., Briffa K.R., Tett, S.F.B., Jones, P.D. & Trigo, R.M. 1999 Evaluation of the
829 North Atlantic Oscillation as simulated by a coupled climate model. Climate
830 Dynamics 15, 685-702.

831 Opsahl, S., Benner, R. & Amon, R.M.W. 1999. Major flux of terrigenous dissolved organic
832 matter through the Arctic Ocean. Limnology and Oceanography 44, 2017-2023.

833 Ostermann, D.R. & Curry, W.B. 2000. Calibration of stable isotopic data: An enriched $\delta^{18}O$
834 standard used for source gas mixing detection and correction. Paleoceanography 15,
835 353-360.

836 Ottersen, G. & Stenseth, N.C. 2001. Atlantic climate variability governs oceanographic and
837 ecological variability in the Barents Sea. Limnology and Oceanography 46, 1774-
838 1780.

839 Ottersen, G. Planque, B. Belgrano A., Post, E., Reid, P.C. & Stenseth, N.C. 2001. Ecological
840 effects of the North Atlantic Oscillation. Oecolgica 128, 1-14.

841 Pannella, G. 1971. Fish otoliths: daily growth layers and periodical patterns. Science 173,
842 1124-1127.

843 Perry, A.L., Low, P.J., Ellis, J.R. & Reynolds, J.D. 2005. Climate change and distribution
844 shifts in marine fisheries. Science 308, 1912-1915.

845 Peterson, B.J., Holmes, R.M., McClelland, J.W., Vörösmarty, C.J., Lammers, R.B.,
846 Shiklomanov, A.I., Shiklomanov, I.A. & Rahmstorf, S. 2002. Increasing river
847 discharge to the Arctic Ocean. Science 298, 2171-2173.

848 Reid, P.C., Planque, B. & Edwards, M. 1998. Is observed variability in long-term results of
849 the Continuous Plankton Recorder survey a response to climate change? Fisheries
850 Oceanography 7, 282-288.

851 Renaud, P., Morata, N., Carroll, M.L., Denisenko, S.G. & Reigstad, M. 2008. Pelagic-benthic
852 coupling in the western Barents Sea: processes and time-scales. Deep-Sea Research II
853 55, 2372-2380, doi:10.1016/j.dsr2.2008.05.017

854 Rhoads, D.C. & Lutz, R.A. (eds.). 1980. Skeletal Growth of Aquatic Organisms: Biological
855 Records of Environmental Change. Plenum Press, New York, 750 pp.

856 Richardson, A.J. & Schoeman, D.S. 2004. Climate impact on plankton ecosystems of the
857 North Atlantic. Science 305, 1609-1612.

858 Richardson, C.A. 2001. Molluscs as archives of environmental change. Oceanography and
859 Marine Biology: An Annual Review 39, 103-164.

860 Sakshaug, E. 1997. Biomass and productivity distrubutions and their variability in the Barents
861 Sea. ICES Journal of Marine Science 54, 341-350.

862 Schöne, B.R., Lega, J., Flessa, K.W.,Goodwin, D.H. & Dettman, D.L. 2002. Reconstructing
863 daily temperatures from growth rates of the intertidal bivalve mollusk *Chione cortezi*
864 (northern Gulf of California, Mexico). Palaeogeography, Palaeoclimatology,
865 Palaeoecology 184, 131-146.

866 Schöne, B.R., Freyre Castro, A.D., Fiebig, J., Houk, S.D., Oschmann, W. & Kröncke, I. 2004.
867 Sea surface water temperatures over the period 1884–1983 reconstructed from oxygen
868 isotope ratios of a bivalve mollusk shell (*Arctica islandica*, southern North Sea)
869 Palaeogeography, Palaeoclimatology, Palaeoecology 212, 215– 232.

870 Schöne, B.R., Houk, S.D., Freyre Castro, A.D., Fiebig, J., Oschmann, W., Kröncke, I.,
871 Dreyer, W. & Gosselck, F. 2005. Daily growth rates in shells of *Arctica islandica*:
872 Assessing sub-seasonal environmental controls on a long-lived bivalve mollusk.
873 Palaios 20, 78-92.

874 Schöne, B.R. 2008. The curse of physiology—challenges and opportunities in the
875 interpretation of geochemical data from mollusk shells. Geo-Marine Letters 28, 269-
876 285.

877 Simstich, J., Harms, I., Karcher, M.J., Erlenkeuser, H., Stanovoy, V., Kodina, L., Bauch, D. &
878 Spielhagen, R.F. 2005. Recent freshening in the Kara Sea (Siberia) recorded by stable
879 isotopes in Arctic bivalve shells. Journal of Geophysical Research 110, C08006,
880 doi:10.1029/2004JC002722.

881 Solomon, C.T., Weber, P.K., Cech Jr., J.J., Ingram, B.L., Conrad, M.E., Machavaram M.V.,
882 Pogodina, A.R. & Franklin, R.L. 2006. Experimental determination of the sources of
883 otolith carbon and associated isotopic fractionation. Canadian Journal of Fisheries and
884 Aquatic Sciences 63: 79–89.

885 Stecher, H.A., Krantz, D.E., Lord, C.J., Luther, G.W. & Bock, K.W. 1996. Profiles of
886 strontium and barium in *Mercenaria mercenaria* and *Spisula solidissima* shells.
887 Geochimica et Cosmochimica Acta 60, 3445-3456.

888 Stein, R., Fahl, K., Fütterer, D.K., Galimov, E.M. & Stepanets, O.V. (eds.). 2003. Siberian
889 river run-off in the Kara Sea: Characterisation, quantification, variability, and
890 environmental significance. Proceedings in Marine Science, Elsevier. 496 pp.

891 Stenseth, N.C., Ottersen, G., Hurrell, J.W. & Belgrano, A. (eds.). 2004. Marine Ecosystems
892 and Climate Variation. The North Atlantic: A comparative perspective. Oxford
893 University Press, 252 pp.

894 Sturgeon, R.E., Willie, S.N., Yang, L., Greenberg, R., Spatz, R.O., Chen, Z., Scriver, C.,
895 Clancy, V., Lam, J.W. & Thorrold, S. 2005. Certification of a fish otolith reference
896 material in support of quality assurance for trace element analysis. Journal of
897 Analytical Atomic Spectrometry 20, 1067-1071.

898 Søreide, J.E., Hop, H., Falk-Petersen, S., Hegseth, E.N. & Carroll, M.L. 2006. Seasonal food
899 web structures and sympagic-pelagic coupling in the European Arctic revealed by
900 stable isotopes and a two-source food web model. Progress in Oceanography 71, 59-
901 87.

902 Tallqvist M.I. & Sundet, J.H. 2000. Annual growth of the cockle *Clinocardium ciliatum* in the
903 Norwegian Arctic (Svalbard area). Hydrobiologia 440, 331-338.

904 Thompson, I., Jones, D.S. & Dreibelbis, D. 1980. Annual internal growth banding and life
905 history of the ocean quahog *Arctica islandica* (Mollusca: Bivalvia). Marine Biology
906 57, 25-34.

907 Thorrold, S.R., Campana, S.E., Jones, C.M. & Swart, P.K. 1997. Factors determining $\delta^{13}C$
908 and $\delta^{18}O$ fractionation in aragonitic otoliths of marine fish. Geochimica et
909 Cosmochimica Acta 61, 2909-2919.

910 Thorrold, S.R., Latkoczy, C., Swart, P.K. & Jones, C.M. 2001. Natal homing in a marine fish
911 population. Science 12, 297-299.

912 Torres, M.E., Barry, J.P., Hubbard, D.A. & Suess E. 2001. Reconstructing the history of fluid
913 flow at cold seep sites from Ba/Ca ratios in vasicomyid clam shells. Limnology and
914 Oceanography 46, 1701-1708.

915 Uvo, C.B. 2003. Analysis and regionalization of northern European winter precipitation based
916 on its relationship with the North Atlantic Oscillation. International Journal of
917 Climatology 23, 1185-1194.

918 Vander Putten, E., Dehairs, F., Keppens, E. & Baeyens, W. 2000. High resolution distribution
919 of trace elements in the calcite shell layer of modern *Mytilus edulis*: Environmental
920 and biological controls. Geochimica et Cosmochimica Acta 64, 997-1011.

921 Vinje, T. & Knambekk, A.S. 1991. Barents Sea drift ice characteristics. Polar Research 10,
922 59-68.

923 Wassmann, P., Reigstad, M., Haug, T., Rudels, B., Carroll, M.L., Hop, H., Gabrielsen, G.W.,
924 Falk-Petersen, S., Denisenko, S.G., Arashkevich, E., Slagstad, D. & Pavlova, O. 2006.
925 Food webs and carbon flux in the Barents Sea. Progress in Oceanography 71, 232-
926 287.

927 Weidman, C.R., Jones, G.A. & Lohmann, K.C. 1994. The long-lived mollusk *Arctica*
928 *islandica*: A new paleoceanographic tool for the reconstruction of bottom
929 temperatures for the continental shelves if the northern North Atlantic Ocean. Journal
930 of Geophysical Research 99, 18305-18314.

931 Witbaard, R., Duineveld, G.C.A. & de Wilde, P.A.W.J. 1999. Geographic differences in
932 growth rates of *Arctica islandica* (Mollsuca: Bivalvia) from the North Sea and
933 adjacent waters. Journal of the Marine Biological Association of the UK 79, 907-915.

934 Xia, J., Ito, E. & Engstrom, D.R. 1997. Geochemistry of ostracode calcite: Part 1. An
935 experimental determination of oxygen fractionation. Geochimica et Cosmochimica
936 Acta 61, 377-382.

937 Ye, H., Ladochy, S., Yang, T., Zhang, T,. Zhang, X. & Ellison, M. 2004. The Impact of
938 Climatic Conditions on Seasonal River Discharges in Siberia. Journal of
939 Hydrometeorology 5, 286.

940 Yoshinaga, J., Nakama, A., Morita, M. & Edmonds, J.S. 2000. Fish otolith reference material
941 for quality assurance of chemical analysis. Marine Chemistry 9, 91-97.

942 Zenkevich, L.1963. Biology of the Seas of the USSR. George Allen & Unwin, London.

7. Figure Captions

Figure 1. Map showing the collection locations of *S. groenlandicus* analyzed for growth rates and stable isotopes/trace elements ((1) is shell 156 and (2) is shell 262), coded for time of collection. The upper map is a larger view of the inset region in the southeast Barents Sea outlined in a bold box. Major river systems, including Severnaya Dvina and Mezen', are shown in the large-scale map.

Figure 2. Schematic showing the timeframe represented by each of the 15 individual *S. groenlandicus* analyzed for growth patterns. Lifespan was determined from the collection date of the individuals and an analysis of the annual growth increments on the shell. Astericeses mark individuals sampled for stable isotope and elemental ratios.

Figure 3. Photo a portion of the cross-section of shell 156, showing the pattern of micromill drill holes. Adjacent holes were drilled along the axis of shell growth and pooled to obtain enough material for stable isotopic analysis. This photo shows 7 sets of pooled samples over 1+ years of growth and 2 growth lines.

Figure 4. Temporal SGI patterns of S. groenlandicus over the 3 collection periods (1899, 1926/1927, and 1968), and combined on a single time scale. The dashed line in each plot represents an SGI of 1.0, with values above this line indicating better than expected years of growth, and values below the line reflecting less than expected growth for those years. Error bars (±1SD) are shown when the sample size exceeded 1 individual; error bars are excluded on the combined plot to enhance readability of patterns.

968 Figure 5. Stable oxygen and carbon isotope profiles of *S. groenlandicus* specimens from (A)
969 1907-1922 (shell 156) and (B) 1946-1959 (shell 262). The vertical dashed lines represent the
970 annual growth bands identified in shell cross-section. Stable isotopes are plotted with the most
971 enriched values at the top of the y-axis.
972
973 Figure 6. Shell profiles of (A) Mn/Ca and Ba/Ca (μmol mol^{-1}) and (B) Sr/Ca and Mg/Ca
974 ratios (mmol mol^{-1}) for the *S. groenlandicus* specimen 156, collected in July 1926. Sample
975 distance is measured from the first growth band sampled closest to the ventral margin. The
976 vertical dashed lines represent the annual growth bands identified in shell cross-section.
977
978 Figure 7. Shell profiles of (A) Mn/Ca and Ba/Ca (μmol mol^{-1}) and (B) Sr/Ca and Mg/Ca
979 ratios (mmol mol^{-1}) for the *S. groenlandicus* specimen 262, collected in July 1968. Sample
980 distance is measured from the first growth band sampled closest to the ventral margin. The
981 vertical dashed lines represent the annual growth bands identified in shell cross-section.
982
983 Figure 8. Relationship between the North Atlantic Oscillation Index (NAO) and the
984 Standardized Growth Index for *S. groenlandicus* collected in 1899, 1926/27, and 1968. NAO
985 is calculated in the 12-month period ending in August of the growth year. Lines are least
986 squared results from linear regressions.
987
988 Figure 9. Summer flow (m^3 sec^{-1} x 10^3 for the months of May, June, and July) of the
989 Severnaya Dvina measured at the Ust'-Pinega gauge for the period 1881-1999. Both annual
990 values (thin line) and a 5-year smoothing function (bold line) are shown. Time periods with
991 growth data of *S. groenlandicus* are highlighted grey, and black bars at the bottom plot denote

992 periods with shell stable isotope (bottom bar) and trace element (top bar) results. Data from
993 Roshydromet (Moscow, Russia).
994
995 Figure 10. Relationship between SGI of *S. groenlandicus* and maximum flow of the
996 Severnaya Dvina River from 1884-1898.
997
998 Figure 11. Relationship between river discharge from the Severnaya Dvina and Mezen'
999 Rivers during the month of maximum flow rate in May, and maximum annual Ba/Ca and
1000 ratios recorded in bivalve aragonite from shells collected in 1926. Lines are least squared
1001 results from linear regressions.
1002

Tables and Figures

Table 1. Information on the samples of *Serripes groenlandicus* selected from the LMR-ZIN archive collections from the southern Barents Sea for analysis in this project.

Date Collected (YYYY.MM.DD)	Collection Number	Number Measured	Latitude	Longitude	Depth (m)	Lifespan
1899.07.18	175	4	69° 13.0' N	36° 40.5' E	190	1882-1899
1899.08.08	373 / 370	2	68° 51.0' N	43° 11.3' E	60	1884-1899
1926.07.13	480	2	68° 46.0' N	42° 26.0' E	78	1908-1926
1926.07.13	*156	3	68° 31.0' N	43° 03.0' E	59	1904-1926
1927.07.04	478	1	69° 10.0' N	43° 13.0' E	62	1907-1927
1927.07.09	138	1	68° 20.0' N	41° 08.5' E	76	1922-1927
1968.06.22	*262	1	69° 00.0' N	45° 00.0' E	60	1946-1968
1968.07.01	263	1	70° 30.0' N	41° 30.0' E	70	1948-1968

* Sampled for stable isotope and trace element ratios and isotopes (See Table 2).

Table 2. Information on *S. groenlandicus* analyzed for stable isotope and trace element ratios, the number of samples and years covered. See Figure 1 for location of samples.

Date Collected (YYYY.MM.DD)	Collection Number	Years (samples) for $\delta^{18}O$, $\delta^{13}C$	Years (samples) for trace elements
1926.07.13	156	16 (68)	6 (54)
1968.06.22	262	14 (51)	6 (51)

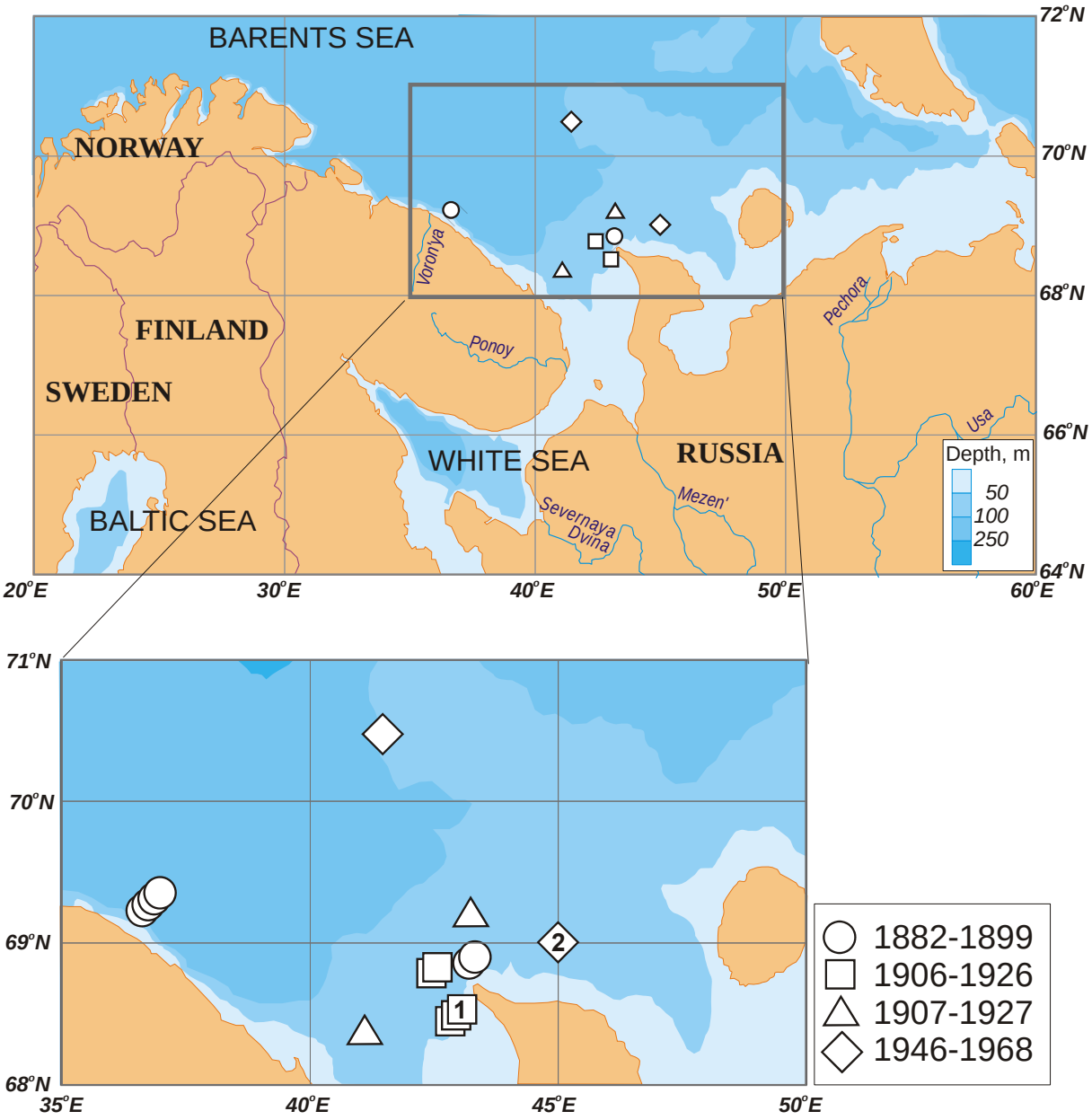

Figure 1. Map showing the collection locations of *S. groenlandicus* analyzed for growth rates and stable isotopes/trace elements ((1) is shell 156 and (2) is shell 262), coded for time of collection. The upper map is a larger view of the inset region in the southeast Barents Sea outlined in a bold box. Major river systems, including Severnaya Dvina and Mezen', are shown in the large-scale map.

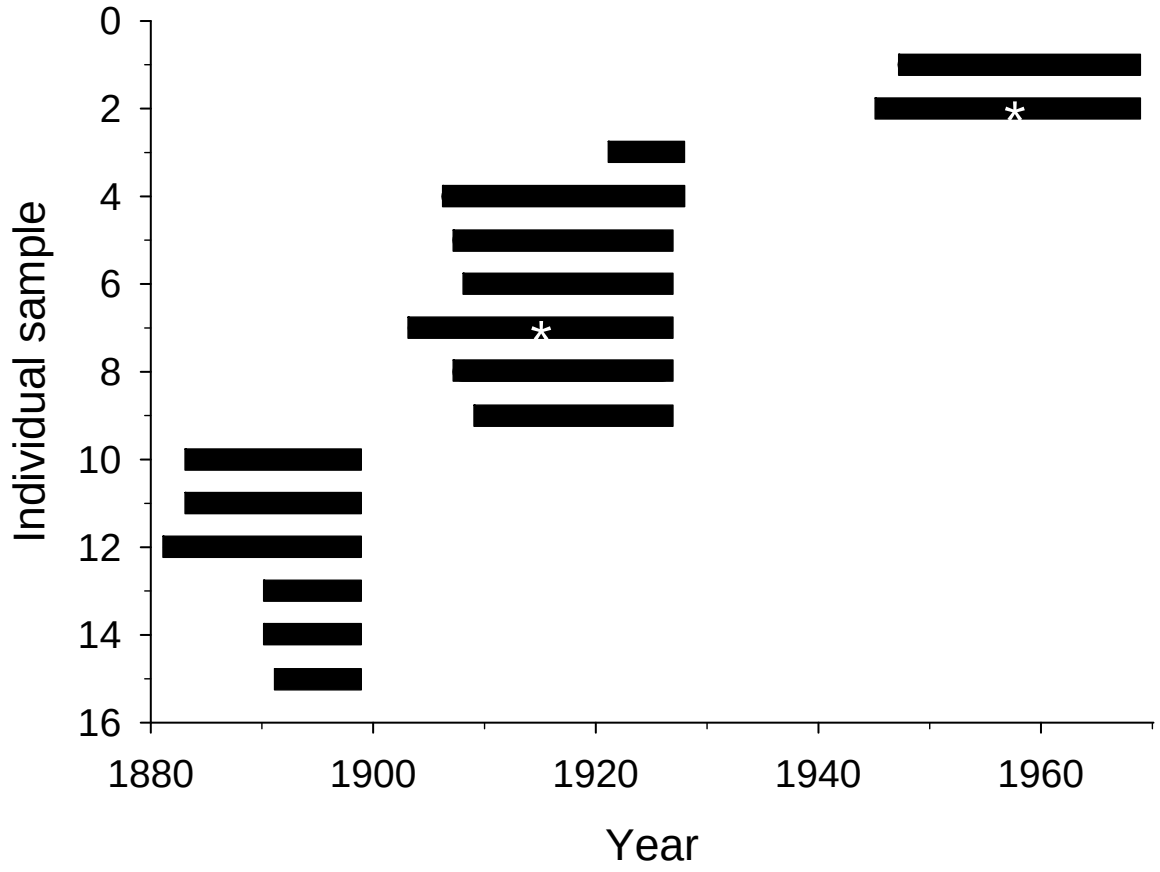

Figure 2. Schematic showing the timeframe represented by each of the 15 individual *S. groenlandicus* analyzed for growth patterns. Lifespan was determined from the collection date of the individuals and an analysis of the annual growth increments on the shell. Asterices mark individuals sampled for stable isotope and elemental ratios.

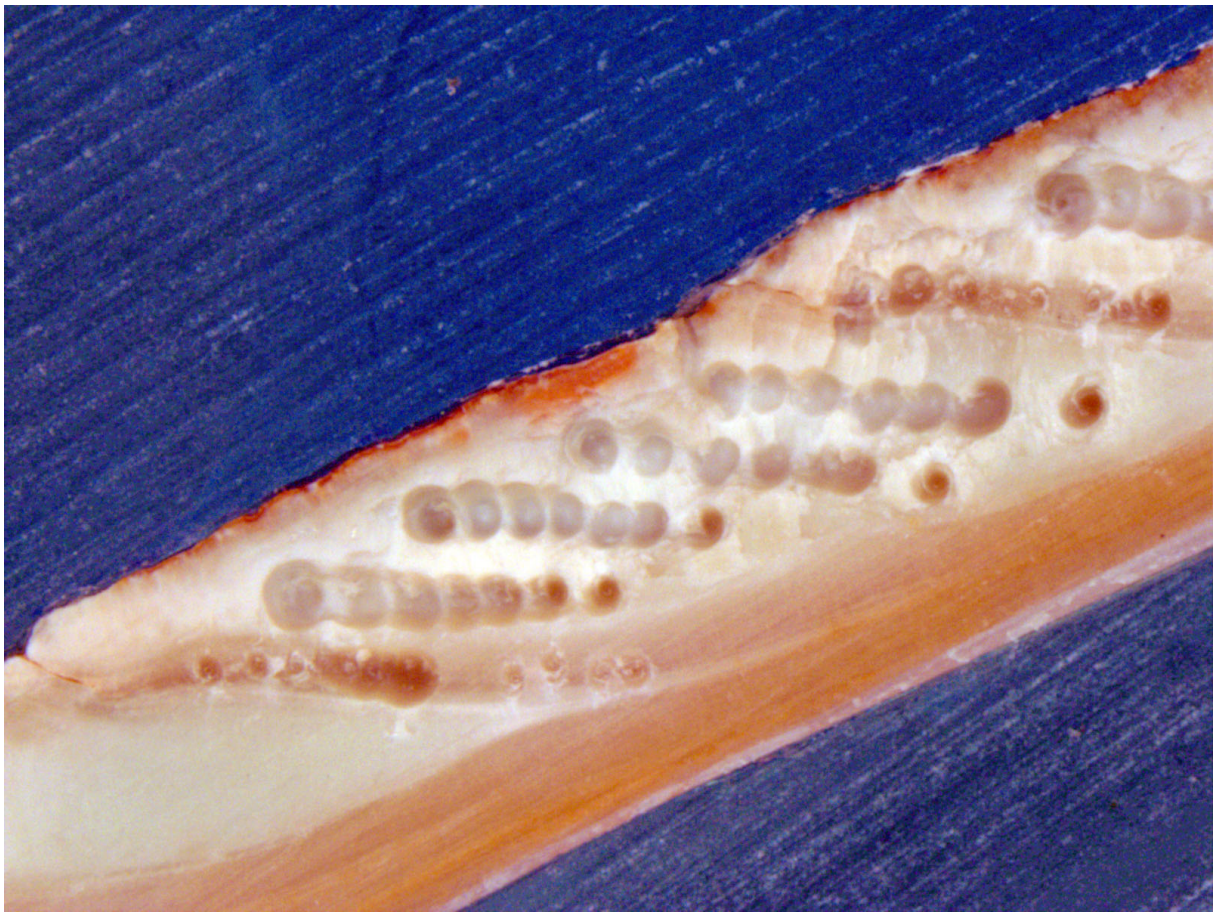

Figure 3. Photo a portion of the cross-section of shell 156, showing the pattern of micromill drill holes. Adjacent holes were drilled along the axis of shell growth and pooled to obtain enough material for stable isotopic analysis. This photo shows 7 sets of pooled samples over 1+ years of growth and 2 growth lines.

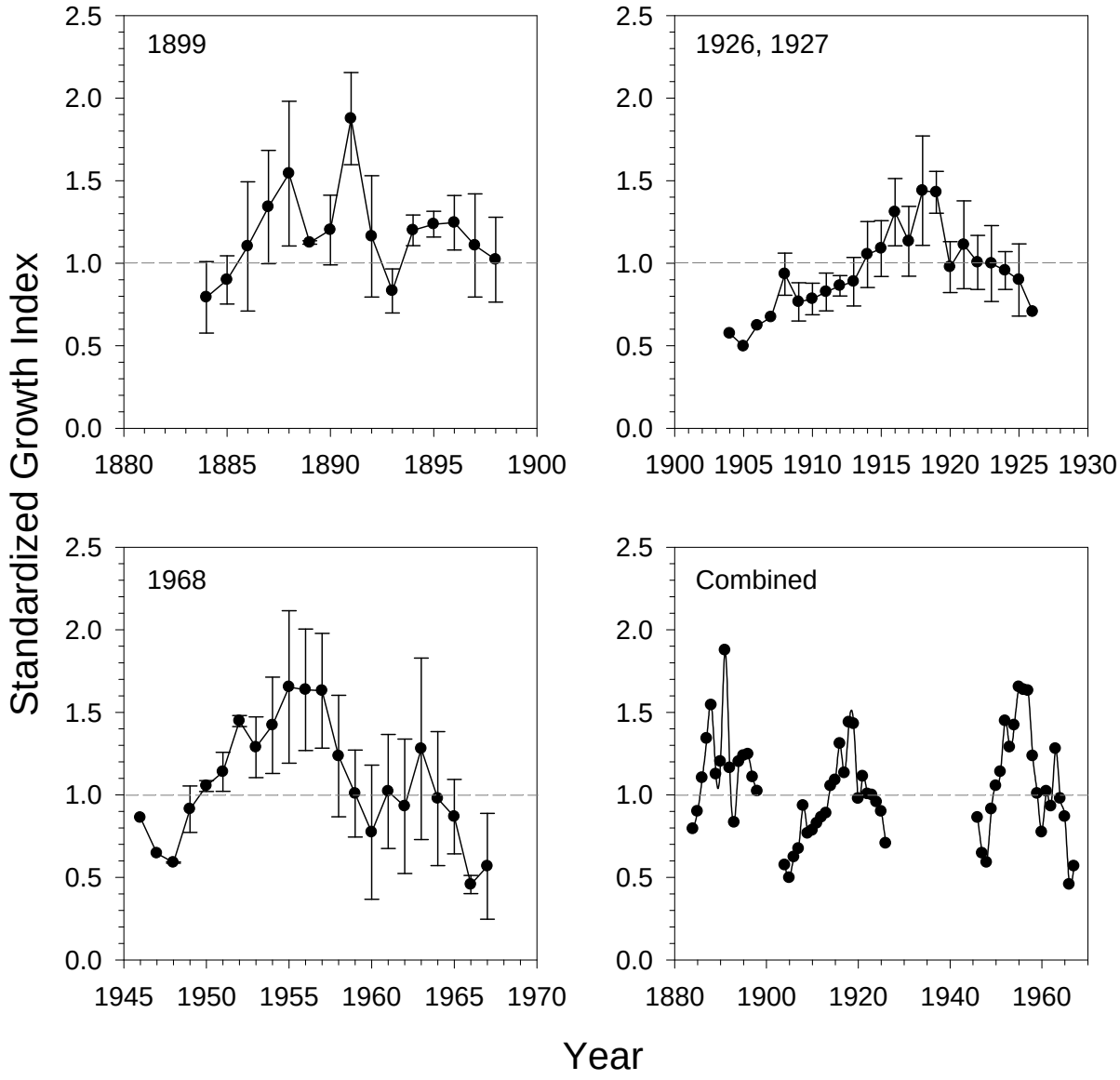

Figure 4. Temporal SGI patterns of *S. groenlandicus* over the 3 collection periods (1899, 1926/1927, and 1968), and combined on a single time scale. The dashed line in each plot represents an SGI of 1.0, with values above this line indicating better than expected years of growth, and values below the line reflecting less than expected growth for those years. Error bars (±1SD) are shown when the sample size exceeded 1 individual; error bars are excluded on the combined plot to enhance readability of patterns.

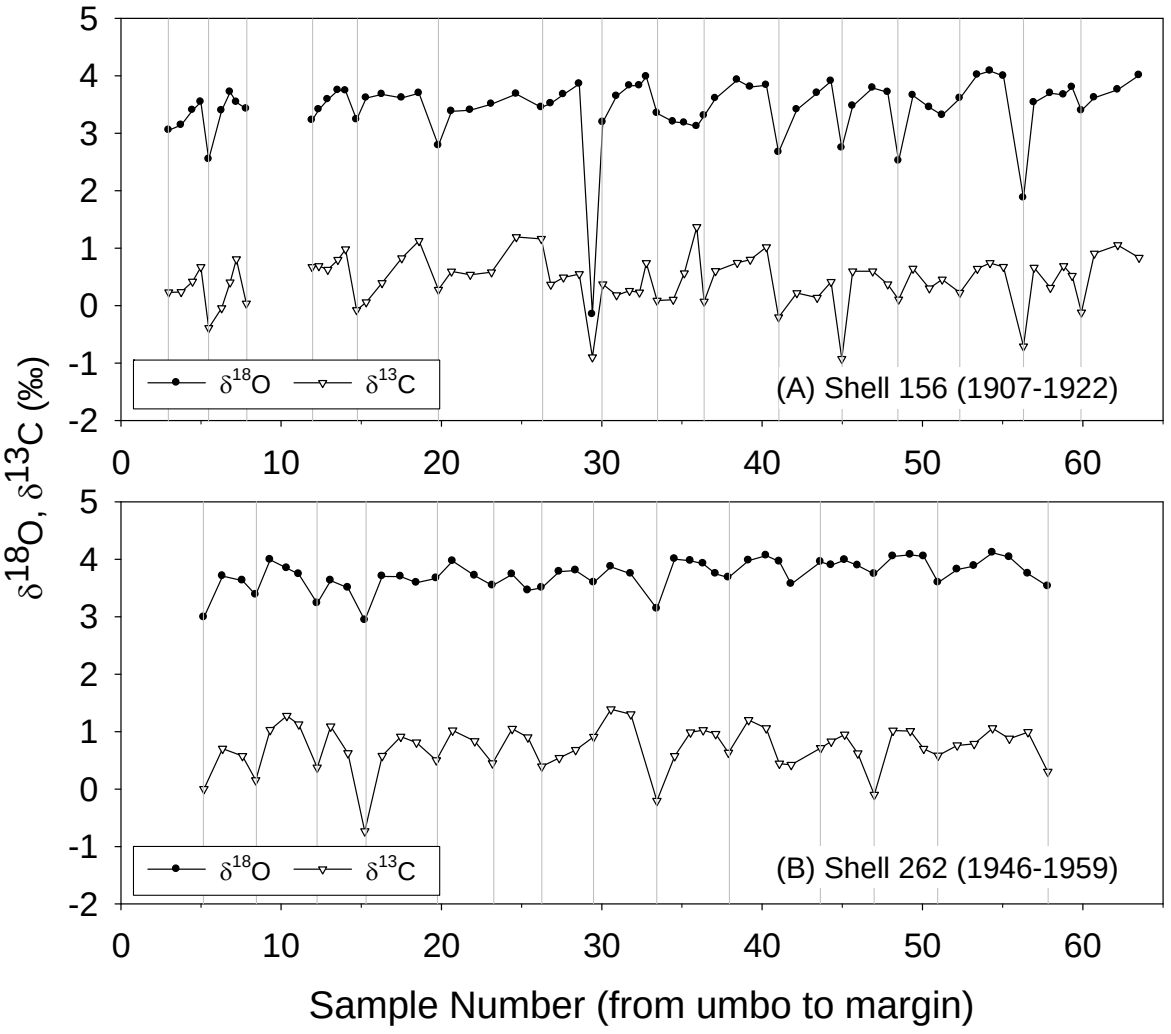

Figure 5. Stable oxygen and carbon isotope profiles of *S. groenlandicus* specimens from (A) 1907-1922 (shell 156) and (B) 1946-1959 (shell 262). The vertical dashed lines represent the annual growth bands identified in shell cross-section. Stable isotopes are plotted with the most enriched values at the top of the y-axis.

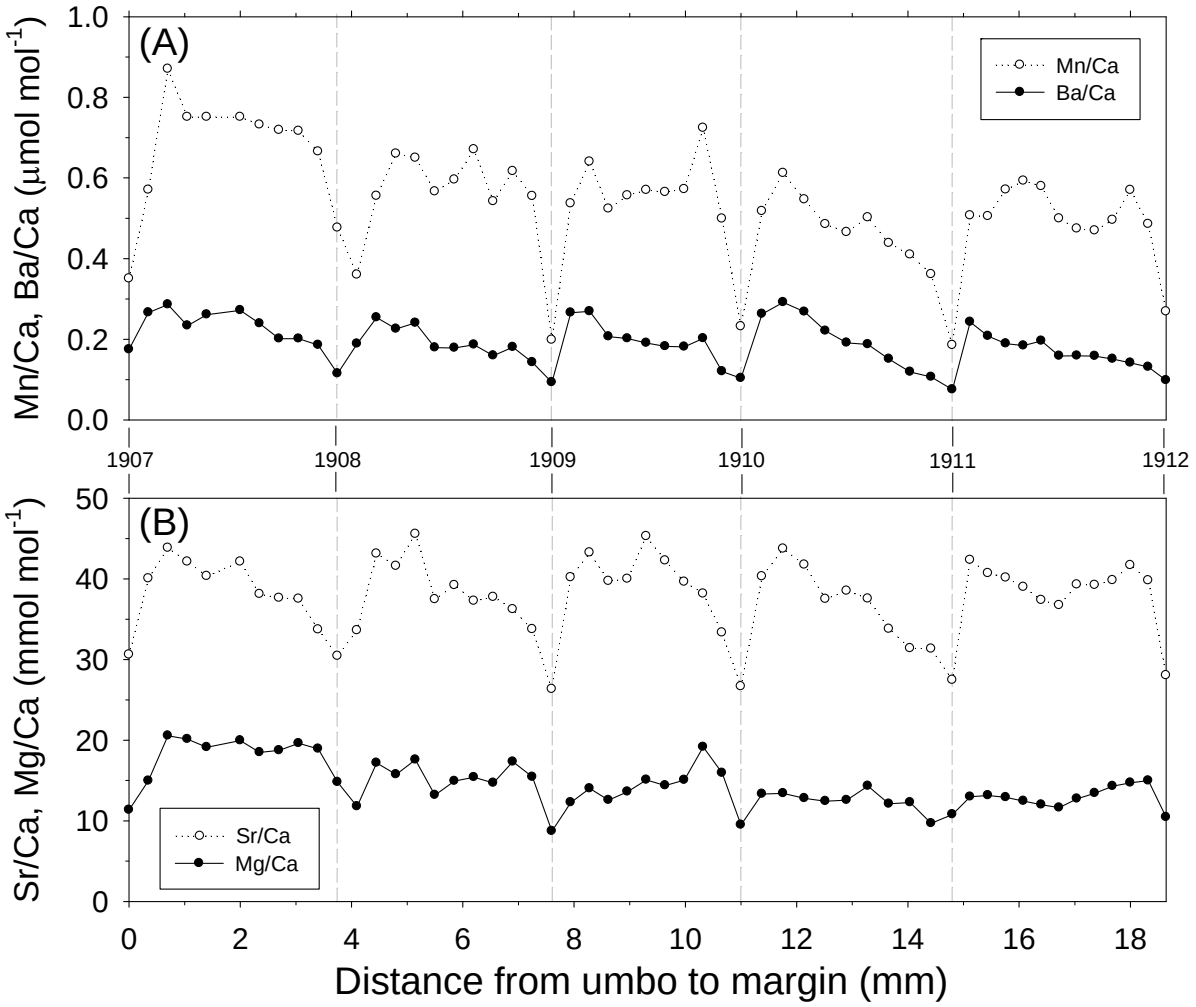

Figure 6. Shell profiles of (A) Mn/Ca and Ba/Ca (µmol mol^{-1}) and (B) Sr/Ca and Mg/Ca ratios (mmol mol^{-1}) for the *S. groenlandicus* specimen 156, collected in July 1926. Sample distance is measured from the first growth band sampled closest to the umbo. The vertical dashed lines represent the annual growth bands identified in shell cross-section.

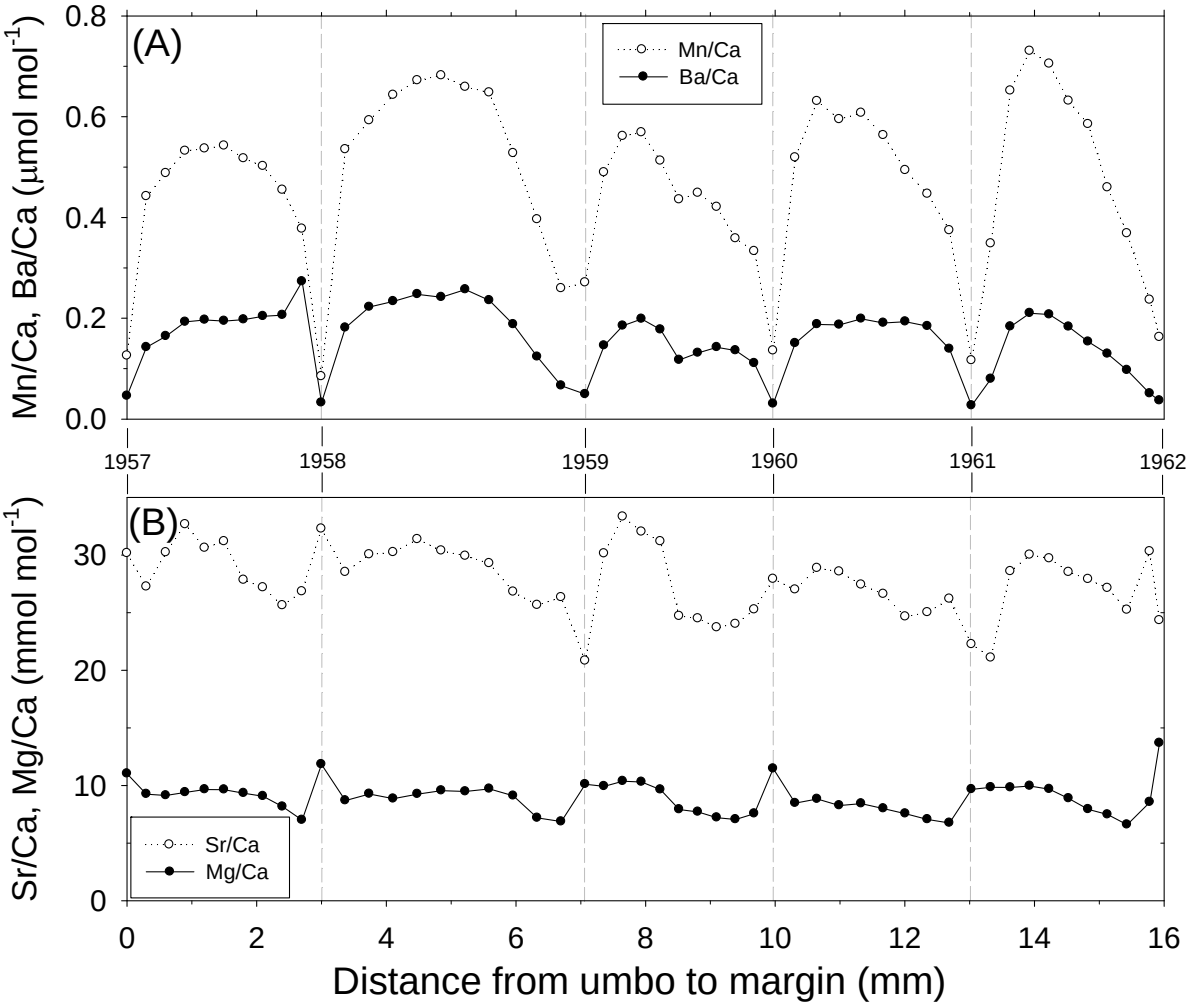

Figure 7. Shell profiles of (A) Mn/Ca and Ba/Ca (µmol mol^{-1}) and (B) Sr/Ca and Mg/Ca ratios (mmol mol^{-1}) for the *S. groenlandicus* specimen 262, collected in July 1968. Sample distance is measured from the first growth band sampled closest to the umbo. The vertical dashed lines represent the annual growth bands identified in shell cross-section.

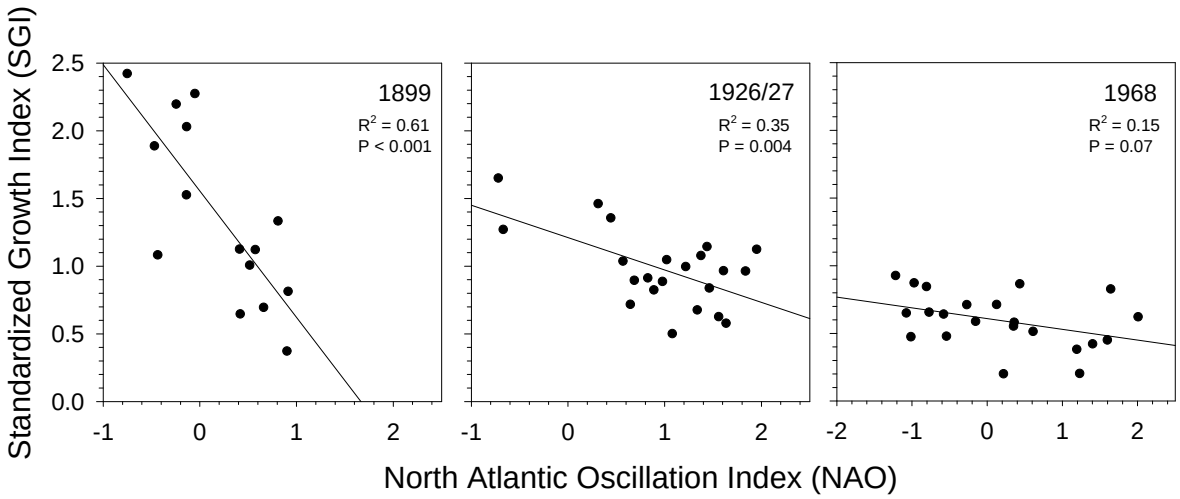

Figure 8. The relationship between the North Atlantic Oscillation Index (NAO) and the Standardized Growth Index for *S. groenlandicus* collected in 1899, 1926/27, and 1968. NAO is calculated in the 12-month period ending in August of the growth year. Lines are least squared results from linear regressions.

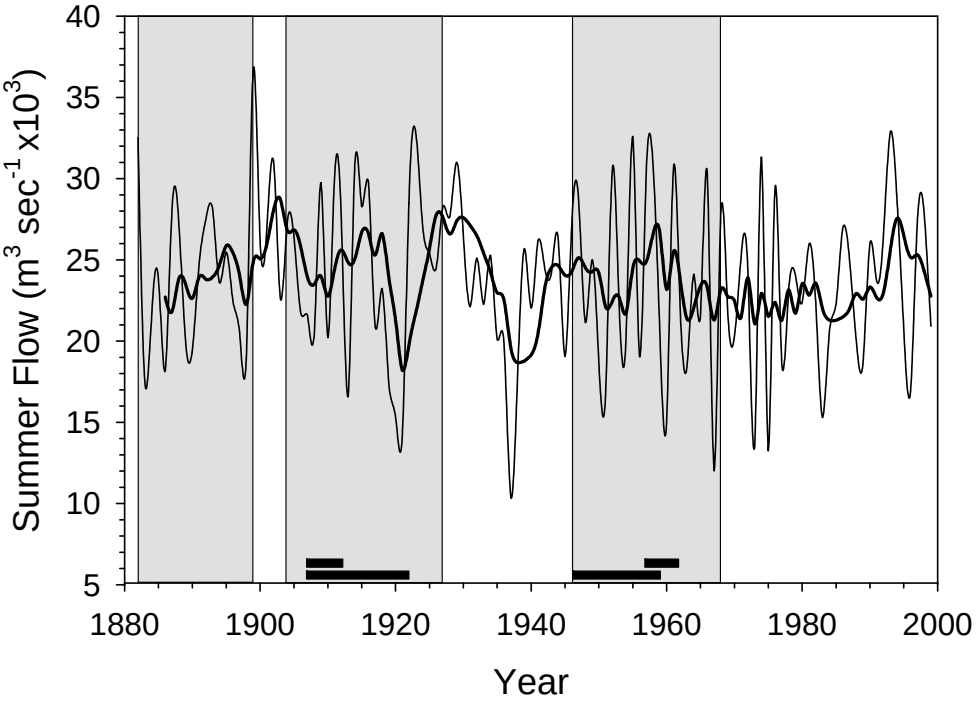

Figure 9. Summer flow (m^3 sec^{-1} x 10^3 for the months of May, June, and July) of the Severnaya Dvina measured at the Ust'-Pinega gauge for the period 1881-1999. Both annual values (thin line) and a 5-year smoothing function (bold line) are shown. Time periods with growth data of *S. groenlandicus* are highlighted grey, and black bars at the bottom plot denote periods with shell stable isotope (bottom bar) and trace element (top bar) results. Data from Roshydromet (Moscow, Russia).

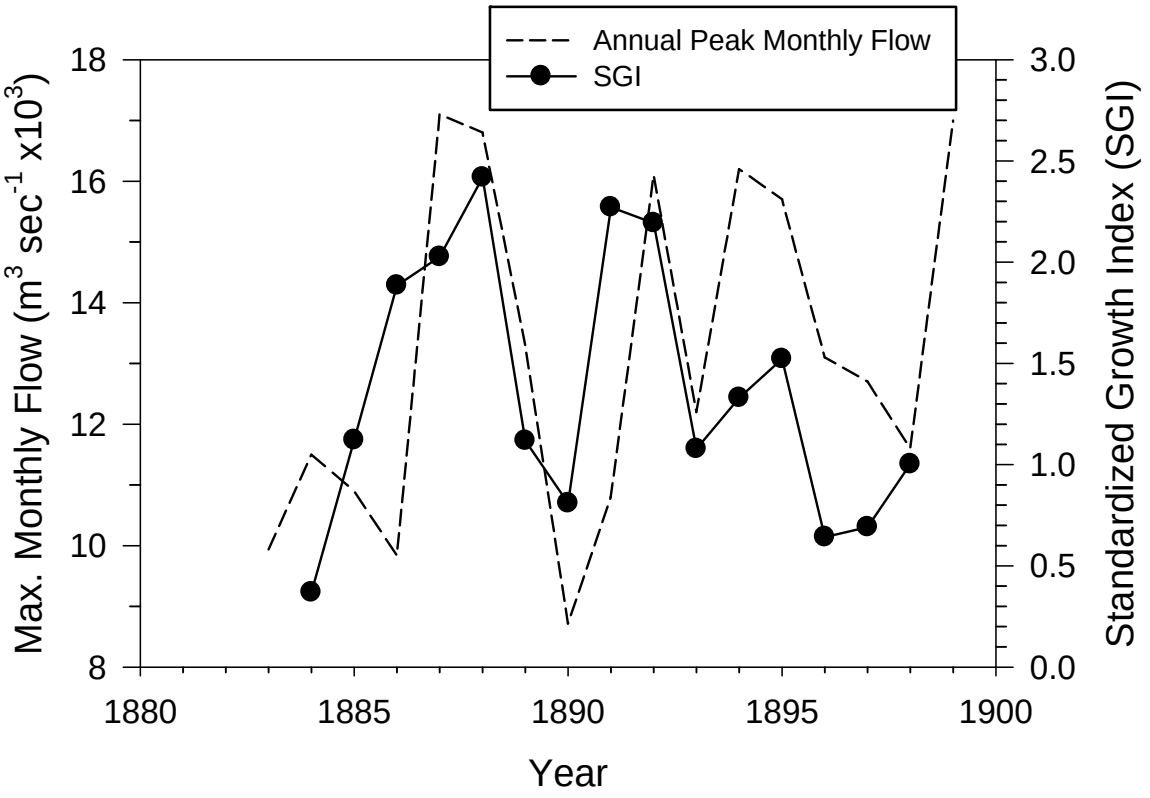

Figure 10. Relationship between SGI of *S. groenlandicus* and maximum flow of the Severnaya Dvina River from 1884-1898.

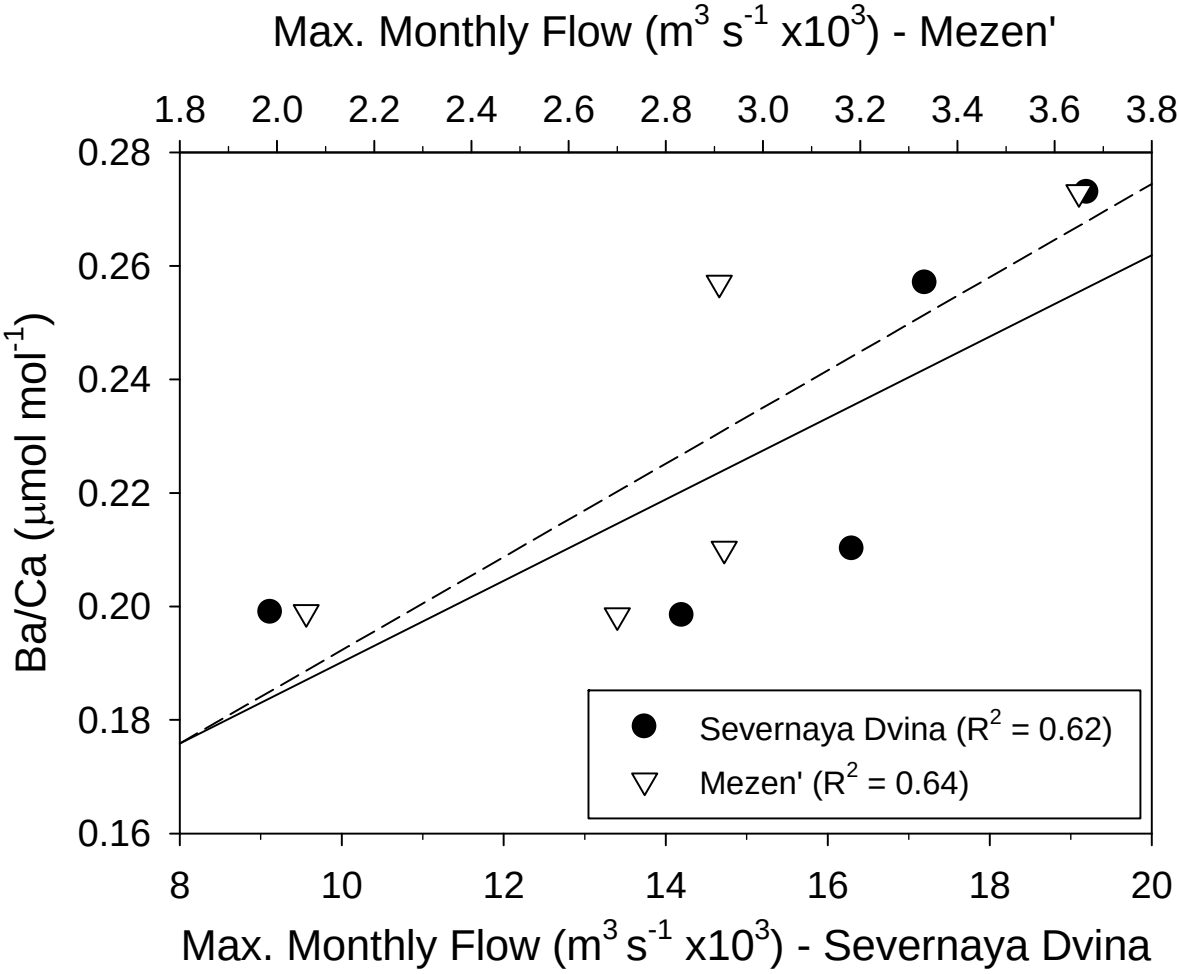

Figure 11. Relationship between river discharge from the Severnaya Dvina and Mezen' Rivers during the month of maximum flow rate in May, and maximum annual Ba/Ca and ratios recorded in bivalve aragonite from shells collected in 1926. Lines are least squared results from linear regressions.